PHILOSOPHICAL TRANSACTIONS OF THE ROYAL SOCIETY A MATHEMATICAL, PHYSICAL & ENGINEERING SCIENCES

A Nonlinear Oscillator with a Strange Attractor

P. Holmes

Phil. Trans. R. Soc. Lond. A 1979 **292**, 419-448
doi: 10.1098/rsta.1979.0068

A NONLINEAR OSCILLATOR WITH A STRANGE ATTRACTOR

By P. HOLMES
Department of Theoretical and Applied Mechanics, Thurston Hall, Cornell University, Ithaca, N.Y. 14853, U.S.A.

(*Communicated by E. C. Zeeman, F.R.S.* – *Received* 21 *August* 1978 – *Revised* 18 *December* 1978)

CONTENTS

Vol. 292. A 1394 41 [Published 23 October 1979

We study the nonlinear oscillator

$$\ddot{x} + \delta\dot{x} - \beta x + \alpha x^3 = f\cos(\omega t) \qquad \text{(A)}$$

from a qualitative viewpoint, concentrating on the bifurcational behaviour occurring as $f \geqslant 0$ increases for α, β, δ, ω fixed > 0. In particular, we study the global nature of attracting motions arising as a result of bifurcations. We find that, for small and for large f, the behaviour is much as expected and that the conventional Krylov–Bogoliubov averaging theorem yields acceptable results. However, for a wide range of moderate f extremely complicated non-periodic motions arise. Such motions are called strange attractors or chaotic oscillations and have been detected in previous studies of autonomous o.d.es of dimension $\geqslant 3$. In the present case they are intimately connected with homoclinic orbits arising as a result of global bifurcations. We use recent results of Mel'nikov and others to prove that such motions occur in (A) and we study their structure by means of the Poincaré map associated with (A). Using analogue and digital computer simulations, we provide a fairly complete characterization of the strange attractor arising for moderate f. This ergodic motion arises naturally from the deterministic differential equation (A).

1. Introduction: a problem in nonlinear vibrations

Techniques such as averaging (the Krylov–Bogoliubov method), harmonic balance or equivalent linearization are often used in nonlinear vibration problems. One of the aims of this paper is to show that such methods can fail to detect, or at best obscure, important behaviour. In particular, when the small parameter conditions are not met, then solutions obtained by averaging can be grossly in error qualitatively as well as quantitatively. However, our main aim is to give an example of a simple forced oscillator which possesses 'strange' solutions (Holmes 1977*b*), solutions which depend on initial conditions in a particularly delicate manner and which behave in an apparently random or chaotic way. We stress that the system in which this behaviour occurs is deterministic and that solutions are stable in the sense that large (transient) disturbances die out after sufficient time and all solution curves $x(t)$ approach a domain A in the state space as $t \to \infty$. A appears to contain an attracting set S which has an extremely complex structure. Sets such as S are called *strange attractors* (Guckenheimer 1976; Holmes 1977*b*); they have previously been detected in problems of population dynamics (May 1974), fluid dynamics (Lorenz 1963, 1964; Ruelle & Takens 1971; Baker *et al.* 1971; Hénon 1976) and in models of the Earth's magnetic field (Cook & Roberts 1970; Robbins 1977) and they are currently the subject of much interest among mathematicians. The author's paper (Holmes 1977*b*) provides a simple introduction to some of this work, which draws on recent developments in differentiable dynamics (Chillingworth 1976; Markus 1971; Smale 1967).

In this paper we study S from two viewpoints. In part I (§§ 2 and 3) we consider the ordinary differential equation (o.d.e.) of the oscillator and prove that homoclinic orbits arise for certain parameter conditions. These predictions are then compared with analogue computer simulations. We also discuss the limitations of the conventional averaging method. With the analogue computer we produce plots of the Poincaré map associated with the oscillator and are thus able to study the structure of S in terms of a two dimensional mapping rather than a three dimensional vector field.

We note that a number of other workers, notably Hayashi *et al.* (1969, 1970, 1973), Ueda *et al.* (1973) and Tondl (1976) have also used these techniques. However, their results have

not been fully discussed nor always interpreted correctly (Holmes 1976). This prompts the second part of our work (§§ 4 and 5) in which we construct and study a simple difference equation which shares much of the behaviour of the Poincaré map. In fact, it appears possible to capture the bulk of the behaviour in a one dimensional mapping. Previous studies of o.d.es with strange solutions (Guckenheimer 1976, 1978; Rand 1978; Williams 1978) and in particular of the Lorenz equation (Lorenz 1963) have used such reduction to one and two dimensional maps, the properties of which are more easily understood. For previous work in mechanics, see the papers of Hsu *et al.* (1975, 1977*a*, *b*). We conclude with comments on the physical implications of the work.

1.1. *A physical problem*

The equation studied in this paper has physical relevance as the simplest possible model of a buckled beam undergoing forced lateral vibrations. The partial differential equation governing such motions, obtained by standard methods, can be written in non-dimensional form as

$$v^{\mathrm{iv}} + \Gamma v'' - K\left[\int_0^1 (v'(\xi))^2 \,\mathrm{d}\xi\right] v'' + \delta\dot{v} + \ddot{v} = P(x, t), \tag{1.1}$$

where $v = v(z, t)$ is the lateral deflexion, a prime denotes differentiation by z and a dot differentiation by t, δ represents viscous damping, K represents the nonlinear membrane stiffness and Γ is the axial compressive load applied to the beam (cf. Huang & Nachbar (1968) for derivation of the equation). The nonlinear term expresses the fact that the axial force in the beam increases with lateral deflexion, leading to increased restoring forces. We assume simply supported boundaries ($v = v'' = 0$ at $z = 0, 1$) and that $\Gamma > \pi^2$, the first Euler load, so that the beam takes up a stable buckled state at rest when the lateral force, P, is zero. Our main simplification involves the assumption that the force $P(x, t)$ has a sinusoidal spatial distribution coinciding with the first mode of the beam and that the time dependence is also sinusoidal. Thus, by writing

$$P(x, t) = f\cos(\omega t)\sin(\pi z),\ v(z, t) = \sum_{i=1}^{N} x_i(t)\sin(\pi z), \tag{1.2}$$

and carrying out the conventional Galerkin averaging we obtain a set of N second order o.d.es, coupled in the nonlinear terms only. Taking just the first of these (constraining $x_j = 0$; $= 2, \ldots, N$) we obtain the equation studied below

$$\ddot{x} + \delta\dot{x} - \beta x + \alpha x^3 = f\cos(\omega t), \tag{1.3}$$

where $$\beta = \pi^2(\Gamma - \pi^2) \quad \text{and} \quad \alpha = \tfrac{1}{2}K\pi^4.$$

Note that this is Duffing's equation with *negative* linear stiffness, since $\Gamma > \pi^2$.

We should stress that (1.3) is only an approximate model for the physical problem outlined, and that all higher modes will be excited by $P(t)$ through the nonlinear coupling. However, we can expect these modal contributions to be small in comparison with the first mode and thus we might expect (1.3) to provide a reasonable model, at least for Γ close to π^2 and f fairly small. It may in fact be possible to show that (1.3) captures all the important behaviour in a qualitative sense in this parameter range. For $f = 0$ a more complex problem of panel flutter has been treated (Holmes 1977*a*; Holmes & Marsden 1978*a*) in which centre manifold theory (Marsden & McCracken 1976) is used to obtain a model similar to (1.3) from the full partial differential equation. Similarly, static loads ($P(x, t) = P_0 + f(t)\,p(x)$) and additional

structural damping might be included. For our study we take (1.3) as the simplest system of this type which displays strange solutions; we can certainly expect other, more complex models to display behaviour at least as complicated (cf. Holmes 1979).

2. Theoretical analysis

2.1. *General properties: global attraction*

We first consider the equations

$$\left.\begin{aligned} \dot{x}_1 &= x_2, \\ \dot{x}_2 &= \beta x_1 - \delta x_2 - \alpha x_1^3, \\ \beta, \delta, \alpha &> 0; \end{aligned}\right\} \tag{2.1}$$

i.e. (1.3) without external forcing. It is simple to check that (2.1) possesses three fixed points at $(0, 0)$ and $(\pm(\beta/\alpha)^{\frac{1}{2}}, 0)$, the latter two being sinks with eigenvalues $\lambda_{1,2} = \frac{1}{2}(-\delta \pm (\delta^2 - 8\beta)^{\frac{1}{2}})$, and the origin a saddle point with $\lambda_{1,2} = \frac{1}{2}(-\delta \pm (\delta^2 + 4\beta)^{\frac{1}{2}})$. All three points have eigenvalues with non-zero real parts (hyperbolic fixed points) and, since it can be shown that there are no other critical elements such as closed orbits in the vector field of (2.1), the system is (topologically) structurally stable (Chillingworth 1976). Linearization and calculation of eigenvalues provides local stability conditions, but for global stability we must seek an appropriate Liapunov function (Hirsch & Smale 1974).

We first rewrite (2.1) in terms of deviations from the two stable sinks:

$$\left.\begin{aligned} \dot{y}_1 &= y_2, \\ \dot{y}_2 &= -2\beta y_1 - \delta y_2 \pm 3(\alpha\beta)^{\frac{1}{2}} y_1^2 - \alpha y_1^3 \quad (y_1 = x_1 \pm (\alpha/\beta)^{\frac{1}{2}},\ y_2 = x_2), \end{aligned}\right\} \tag{2.2}$$

and we take as a Liapunov function

$$V = \tfrac{1}{2}y_2^2 + \beta y_1^2 + \tfrac{1}{4}\alpha + \nu(\tfrac{1}{2}\delta y_1^2 + y_1 y_2).$$

It is easy to check that this is globally positive definite and increasing with $(y_1^2 + y_2^2)^{\frac{1}{2}}$ for all $0 < \nu < \delta$. Differentiating V along solution curves of (2.2), we obtain

$$\mathrm{d}V/\mathrm{d}t = -(\delta - \nu)\, y_2^2 - 2\nu\beta y_1^2 \pm 3\nu(\alpha\beta)^{\frac{1}{2}} y_1^3 \pm 3(\alpha\beta)^{\frac{1}{2}} y_1^2 y_2 - \alpha\nu y_1^4.$$

Clearly if y_1 and y_2 are sufficiently large then the $-\alpha\nu y_1^4$ and $-(\delta - \nu)\, y_2^2$ terms dominate the $3(\alpha\beta)^{\frac{1}{2}}(\nu y_1 + y_2)\, y_1^2$ term and choosing $\nu \in (0, \delta)$, we have $\mathrm{d}V/\mathrm{d}t \leqslant 0$. Thus solutions of (2.2), and hence of (2.1), remain bounded for all time and approach and enter a bounded set $A \subset \mathbb{R}^2$. To show that almost all solutions actually approach one or other of the sinks at $(\pm(\alpha/\beta)^{\frac{1}{2}}, 0)$ we use a second Liapunov function (actually a pair of functions, one for $(+(\beta/\alpha)^{\frac{1}{2}}, 0)$, one for $(-(\beta/\alpha)^{\frac{1}{2}}, 0)$):

$$V' = \tfrac{1}{2}y_2^2 + \beta y_1^2 \pm 3(\alpha\beta)^{\frac{1}{2}} y_1^3 + \tfrac{1}{4}\alpha y_1^4 + \nu(\tfrac{1}{2}\delta y_1^2 + y_1 y_2).$$

These functions are defined within the two areas enclosed by the loop Γ_0 of figure 3, below, whose equation is

$$H(x_1, x_2) = \tfrac{1}{2}x_2^2 - \tfrac{1}{2}\beta x_1^2 + \tfrac{1}{4}\alpha x_1^4 = 0. \tag{2.3}$$

We thus obtain

$$\frac{\mathrm{d}V'}{\mathrm{d}t} = -(\delta - \nu)\, y_2^2 - 2\nu\beta y_1^2 \pm 3(\alpha\beta)^{\frac{1}{2}} y_1^3 - \nu\alpha y_1^4,$$

which is negative definite inside the loop Γ_0. Thus all solutions starting within Γ_0 approach one or other of the sinks as $t \to +\infty$. It remains to check that there are no attractors *outside* Γ_0.

Since there are no fixed points and the system is planar, the only possibility is a limit cycle. Taking the Hamiltonian energy $H(x_1, x_2)$ of equation (2.3) and differentiating along solutions of (2.1) we obtain $\mathrm{d}H/\mathrm{d}t = -\delta x_2^2$. The energy is therefore decreasing on any closed curve and thus no limit cycles exist. This shows that any solution not starting on the stable manifold Γ^s of the saddle point approaches a sink as $t \to +\infty$, as shown in figure 1.

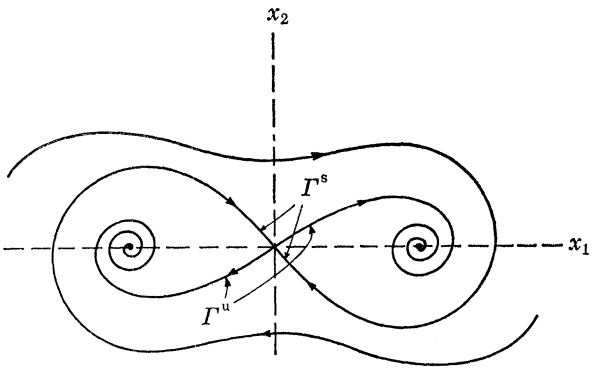

FIGURE 1. The planar vector field for $f \equiv 0$; $\alpha, \beta, \delta > 0$.

We now consider the situation for $f \neq 0$. In this case (1.3) can be rewritten as a first order autonomous o.d.e. on $\mathbb{R}^2 \times S^1$, where $\mathbb{R}^2$ is the (x_1, x_2) plane as above, and $\theta \in S^1$ denotes points on the unit circle:

$$\left.\begin{aligned} \dot{x}_1 &= x_2, \\ \dot{x}_2 &= \beta x_1 - \delta x_2 - \alpha x_1^3 + f\cos\theta, \\ \dot{\theta} &= \omega. \end{aligned}\right\} \tag{2.4}$$

The third component, $\dot{\theta} = \omega$, shows that (2.4) has no fixed points. For small f we can consider (2.4) as a *periodic perturbation* of (2.1) where (2.4) with $f = 0$ represents the trivial case in that behaviour in the (x_1, x_2) plane is identical for all $\theta \in [0, 2\pi/\omega)$. In particular, the fixed points $(0, 0)$ and $(\pm(\beta/\alpha)^{\frac{1}{2}}, 0)$ generate hyperbolic circular closed orbits in $\mathbb{R}^2 \times S^1$. By the invariant manifold theorem (Hirsch *et al.* 1977) orbits persist for (small) $f \neq 0$, losing their circularity but retaining their qualitative features. Thus we expect to obtain two stable attracting orbits 'close' to $(\pm(\beta/\alpha)^{\frac{1}{2}}, 0)$ and a single saddle type orbit close to $(0, 0)$. This is indeed the case (§ 3). Moreover, since (2.1) is a (globally) structurally stable system *we also expect the global structures of the manifolds* Γ^s *and* Γ^u *to be preserved* (Chillingworth 1976; Hirsch *et al.* 1977).

To confirm and extend these results we again use the Liapunov function V', but now differentiate along solution curves of the forced system to obtain

$$\begin{aligned} \mathrm{d}V'/\mathrm{d}t &= -(\delta-\nu)\, y_2^2 - 2\nu\beta y_1^2 \pm 3\nu(\alpha\beta)^{\frac{1}{2}}\, y_1^3 - \nu\alpha y_1^4 + y_2 f\cos(\omega t) + \nu y_1 f\cos(\omega t), \\ &\leqslant -(\delta-\nu)\, y_2^2 - 2\nu\beta y_1^2 \pm 3\nu(\alpha\beta)^{\frac{1}{2}}\, y_1^3 - \nu\alpha y_1^4 + |y_2 f| + |\nu y_1 f|. \end{aligned} \tag{2.5}$$

Setting $f = O(\epsilon^2)$ $(\epsilon \ll 1)$ we can see that if y_1, y_2 are (slightly) greater than $O(\epsilon)$ then we have $\mathrm{d}V'/\mathrm{d}t < 0$. Thus solutions remain bounded and in some neighbourhood of $(y_1, y_2) = (0, 0)$ for small f.

We might also suspect that global stability is preserved for large f. To see that this is the case we return to the first Liapunov function V and differentiate along solution curves of the forced system:

$$\begin{aligned} \mathrm{d}V/\mathrm{d}t &= -(\delta-\nu)\, y_2^2 - 2\nu\beta y_1^2 \pm 3(\alpha\beta)^{\frac{1}{2}}\,(-\nu y_1 + y_2)\, y_1^2 - \alpha\nu y_1^4 + f(\nu y_1 + y_2)\cos(\omega t), \\ &\leqslant -(\delta-\nu)\, y_2^2 - 2\nu\beta y_1^2 + 3(\alpha\beta)^{\frac{1}{2}}\,|y_1^2 y_2| + 3\nu(\alpha\beta)^{\frac{1}{2}}\,|y_1^3| + |\nu y_1 f| + |y_2 f| - \alpha\nu y_1^4. \end{aligned}$$

Again it is clear that $dV/dt < 0$ if we take y_1 and y_2 sufficiently large. Thus for small f solutions tend to remain in either of two regions A_1^f, A_2^f and for large f within the large region A_3^f as shown in figure 2.

Remark. It is possible to obtain analogous global stability criteria for the partial differential equation (1.1) working in a suitable function space setting (Holmes & Marsden 1978*a*; Holmes 1979).

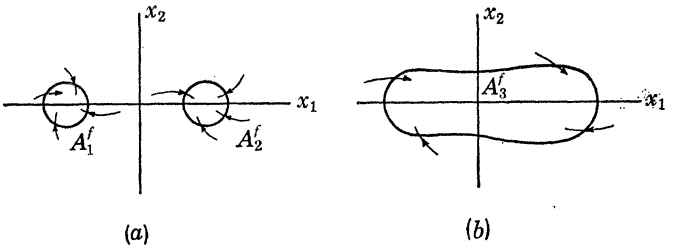

FIGURE 2. Global stability for $f \neq 0$; $\alpha, \beta, \delta, \omega > 0$.
(*a*) Small Force, $f = O(\epsilon^2)$; (*b*) large force.

2.2. *Application of the averaging theorem*

We apply a version of the well known averaging theorems originally due to Krylov and Bogoliubov. This version is due to Hale (1969) and has been stated and used previously in an application to the Duffing equation with positive linear stiffness (Holmes & Rand 1976).

We first employ the transformation $z_1 = x_1 \cos(\omega t) - (x_2/\omega)\sin(\omega t)$, $z_2 = -x_1 \sin(\omega t) - (x_2/\omega)\cos(\omega t)$ with inverse $x_1 = z_1 \cos(\omega t) - z_2 \sin(\omega t)$; $x_2 = -\omega[z_1 \sin(\omega t) + z_2 \cos(\omega t)]$. The transformed system then takes the form of a pair of non-autonomous first order o.d.es.

$$\left.\begin{aligned} z_1 &= \frac{1}{\omega}\{\rho[z_1\cos(\omega t) - z_1\sin(\omega t)] + \alpha[z_1\cos(\omega t) - z_1\sin(\omega t)]^3 \\ &\qquad - \delta\omega[z_1\sin(\omega t) + z_2\cos(\omega t)] - f\cos(\omega t)\}\sin(\omega t), \\ z_2 &= \frac{1}{\omega}\{\rho[z_1\cos(\omega t) - z_1\sin(\omega t)] + \alpha[z_1\cos(\omega t) - z_1\sin(\omega t)]^3 \\ &\qquad - \delta\omega[z_1\sin(\omega t) + z_2\cos(\omega t)] - f\cos(\omega t)\}\cos(\omega t). \end{aligned}\right\} \tag{2.6}$$

Following the averaging theorem we replace the right-hand side of (2.6) by the autonomous functions obtained by averaging for $t \in [0, \infty)$. For periodic functions we simply integrate over $t = 0 \to 2\pi/\omega$. We thus obtain

$$\left.\begin{aligned} \dot{z}_1 &= \tfrac{1}{2}\omega^{-1}\{-\rho z_2 - \delta\omega z_1 - \tfrac{3}{4}\alpha z_2(z_1^2 + z_2^2)\}, \\ \dot{z}_2 &= \tfrac{1}{2}\omega^{-1}\{\rho z_1 - \delta\omega z_2 + \tfrac{3}{4}\alpha z_1(z_1^2 + z_2^2) - f\}, \end{aligned}\right\} \tag{2.7}$$

where $\rho = -\beta - \omega^2$. The approximate solutions provided by (2.7) are valid for all t (Hale 1969), provided that the parameters ρ/ω, α/ω, δ and f/ω of (2.6) are small. Since $\rho = -\beta - \omega^2$, this implies that both β *and* ω must be small.

Now consider the invariant manifold results above: that for small f there are two stable attracting orbits near $(\pm(\beta/\alpha)^{\frac{1}{2}}, 0)$. To study the behaviour of those orbits it is natural to transform the equations so that one of the points (say $(-(\beta/\alpha)^{\frac{1}{2}}, 0)$) lies at the origin:

$$\left.\begin{aligned} \dot{y}_1 &= y_2, \\ \dot{y}_2 &= -2\beta y_1 - \delta y_2 + 3(\alpha\beta)^{\frac{1}{2}} y_1^2 - \alpha y_1^3 + f\cos(\omega t). \end{aligned}\right\} \tag{2.8}$$

Applying the averaging theorem to this system, all quadratic terms vanish and we obtain an expression identical to (2.7) above but with ρ replaced by $\nu = 2\beta - \omega^2$.

If the small parameter conditions noted above are met (with ν replacing ρ as appropriate), then a fixed point solution (z_1', z_2') of (2.7) corresponds to an almost sinusoidal solution of the original system (1.3). More precisely, if we write (2.7) in polar coordinates, $z = (z_1^2 + z_2^2)^{\frac{1}{2}}$, $\theta = \arctan(z_2/z_1)$, we obtain

$$\left.\begin{aligned} \dot{z} &= \tfrac{1}{2}\omega^{-1}\{-\delta\omega z - f\sin\theta\}, \\ \dot{\theta} &= \tfrac{1}{2}\omega^{-1}\{\rho + \tfrac{3}{4}\alpha r^2 - (f/r)\cos\theta\} \quad \text{(replace } \rho \text{ by } \nu \text{ when appropriate).} \end{aligned}\right\} \tag{2.9}$$

A fixed point (z', θ') of (2.9) then corresponds to a solution of (2.4) with average modulus z' and phase θ', $z'\cos(\omega t + \theta')$. Moreover, the stability properties of solutions of the averaged system carry over to the original system (Holmes & Rand 1976) and we can thus study the *bifurcations* in the vector field of (2.4) by examining those of (2.9).

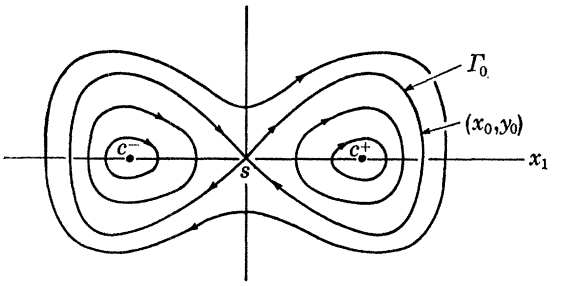

FIGURE 3. The Hamiltonian system $\dot{x}_1 = x_2$, $\dot{x}_2 = \beta x_1 - \alpha x_1^3$. $c^{\pm}$ are centres, s is the saddle point.

In the work below we are particularly interested in behaviour as f is increased from zero for fixed α, β, δ and ω. Physical considerations, supported by our invariant manifold analysis above, suggest that for small f there will be stable oscillations near $(\pm(\beta/\alpha)^{\frac{1}{2}}, 0)$. Physical considerations also suggest that for large f, oscillations will occur which encompass the positions of all three fixed points of the unforced system. It turns out that the former, small force, oscillations are represented reasonably well by the averaged system (2.7) with ρ replaced by ν, and the large force oscillations by (2.7) as it stands (we demonstrate the comparison in § 3, below). However, the main investigation in this paper is for the case of 'medium' f, for which the averaging theorem spectacularly fails. To investigate phenomena that arise in this case we turn to the work of Mel'nikov (1963).

2.3. *Periodic perturbation of an autonomous system with homoclinic orbits*

To apply the methods of Mel'nikov we first rewrite (2.4) as a perturbation of a Hamiltonian system which possesses a 'saddle connection', in this case the four seperatrices leaving and entering the saddle point, which form two loops, the whole being marked Γ_0 in figure 3. The full system is then

$$\left.\begin{aligned} \dot{x}_1 &= x_2, \\ \dot{x}_2 &= \beta x_1 - \alpha x_1^3 + \epsilon(\bar{f}\cos\omega t - \bar{\delta} x_2), \end{aligned}\right\} \tag{2.10}$$

(i.e. we have replaced δ by $\epsilon\bar{\delta}$, f by $\epsilon\bar{f}$ with ϵ small). We note that Morosov (1973, 1976) has studied a similar system, but with positive linear stiffness.

Next consider the Poincaré map P: $\Sigma \to \Sigma$ defined on the cross section $\Sigma = \{(x, y, \theta) \in \mathbb{R}^2 \times S^1 | \theta = \theta_0 \in [0, 2\pi/\omega)\}$ (Chillingworth 1976). Note that, in view of the third component of (2.4), P is defined globally and $\Sigma = \mathbb{R}^2$. Closed orbits of (2.4) correspond to fixed points of P and stability types also carry over. The qualitative structure of P is easily found for the trivial case $\epsilon = 0$. P possess three fixed points at $s = (0, 0)$ and $c^{\pm} = (\pm(\beta/\alpha)^{\frac{1}{2}}, 0)$ and the saddle seperatrix orbits Γ of (2.1) become stable and unstable manifolds M_s^s and M_s^u of the saddle. For $\epsilon = 0$ the manifolds are identified.

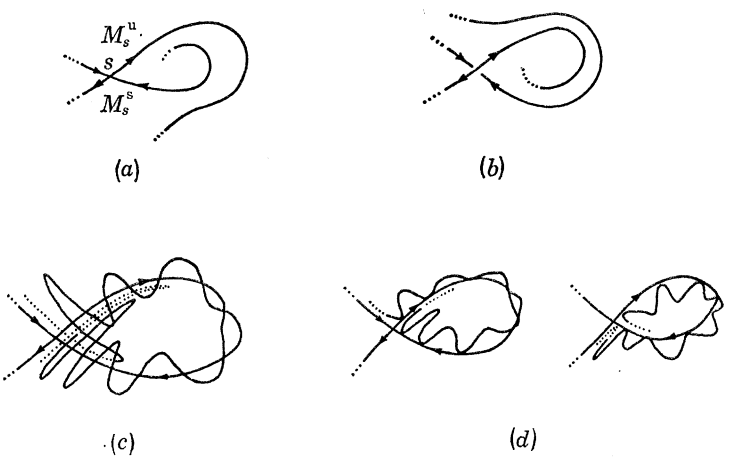

FIGURE 4. The possible structures for stable and unstable manifolds of the saddle point s; (*a*) M_s^u 'outside' M_s^s; $\Delta_\epsilon(t_0) < 0$; (*b*) M_s^u 'inside' M_s^s; $\Delta_\epsilon(t_0) > 0$; (*c*) M_s^u intersects M_s^s transversally; $\Delta_\epsilon(t_0) \lesseqgtr 0$; (*d*) M_s^u 'touches' M_s^s; $\Delta_\epsilon(t_0) \geqslant 0$ or $\Delta_\epsilon(t_0) \leqslant 0$.

Clearly the structure of these manifolds plays an important role in determining the nature of solutions of (2.10), and we shall study this for $\epsilon \neq 0$ by Mel'nikov's methods. In particular, we wish to know how the structurally unstable loops $\Gamma_0 = M_s^s \cap M_s^u$ will break for fixed $\beta, \delta, \alpha, \omega, f$ as ϵ increases. One of three situations will occur (cf. Chillingworth 1976): (1) each loop breaks so that the unstable manifold M_s^u passes 'outside' the stable manifold M_s^s; (2) M_s^u passes 'inside' M_s^s, or (3) M_s^u and M_s^s meet. If they meet they generally do so transversally, although quadratic or higher order contact is possible. Since M_s^s and M_s^u are invariant under P, the existence of one intersection implies the existence of infinitely many. The various cases are shown in figure 4.

Mel'nikov (1963) showed how a function $\Delta_\epsilon(t_0)$ can be derived for systems such as (2.10) so that the value of $\Delta_\epsilon(t_0)$ determines the structure of M_s^u and M_s^s. In particular, if $\Delta_\epsilon(t_0)$ oscillates and takes both positive and negative values then case (*c*) (transversal intersection) occurs. Similarly if $\Delta_\epsilon(t_0) > 0$ (resp. < 0) case (*b*) (resp. (*a*)) occurs and if $\Delta_\epsilon(t_0) \geqslant 0$ (resp. $\leqslant 0$) (i.e. $\Delta_\epsilon(t_0)$ oscillates and (periodically) touches zero) the left (resp. right) hand version of case (*d*) occurs.†

If the perturbed system is expressed in general terms as

$$\left.\begin{aligned} \dot{x} &= p_0(x, y) + \epsilon p_1(x, y, \omega t, \epsilon), \\ \dot{y} &= q_0(x, y) + \epsilon q_1(x, y, \omega t, \epsilon), \end{aligned}\right\} \tag{2.11}$$

† In Mel'nikov's paper there is an inconsistency between the signs in the expression for $\Delta_\epsilon(t_0)$ on page 30 and the figure on page 33; moreover, the condition $p_1(0, 0, \omega t, \epsilon) = q_1(0, 0, \omega t, \epsilon)$ can be relaxed.

where $p_0, \ldots, q_1$ possess certain properties described by Mel'nikov (1963), and in particular the unperturbed system ($\epsilon = 0$) possesses a non-degenerate saddle point at (0, 0), then $\Delta_\epsilon(t_0)$ can be written

$$\Delta_\epsilon(t_0) = -q_0(x_0, y_0)\{x_\epsilon^+(t_0, \omega, t_0) - x_\epsilon^-(t_0, \omega, t_0)\} + p_0(x_0, y_0)\{y_\epsilon^+(t_0, \omega, t_0) - y_\epsilon^-(t_0, \omega, t_0)\}. \quad (2.12)$$

Here the point (x_0, y_0) is chosen to lie on the seperatrix Γ_0 of the unperturbed system (cf. figure 3) with $(x_0, y_0) \neq (0, 0)$ and $(x_\epsilon^\pm(t, \omega, t_0), y_\epsilon^\pm(t, \omega, t_0))$ denote the solution curves of the *perturbed* ($\epsilon \neq 0$) system starting at points $(x_\epsilon^\pm(t_0, \omega, t_0), y_\epsilon^\pm(t_0, \omega, t_0))$ at time t_0 and tending to (0, 0) as $t \to \pm\infty$ respectively. It can be checked that $(x_\epsilon^\pm(t_0, \omega, t_0), y_\epsilon^\pm(t_0, \omega, t_0))$ lie on the normal to the trajectory Γ_0 passing through (x_0, y_0). Thus $\Delta_\epsilon(t_0)$ measures the distance between the two branches of the seperatrices of the perturbed system; i.e. it characterizes the manner in which Γ_0 breaks for $\epsilon \neq 0$. In fact Mel'nikov proves that the solutions $(x_\epsilon^\pm(t, \omega, t_0), y_\epsilon^\pm(t, \omega, t_0))$ do exist for $\epsilon \neq 0$, small, and that the function $\Delta_\epsilon(t_0)$ thus is well defined. Moreover, he shows how $\Delta_\epsilon(t_0)$ can be constructed as a power series in ϵ, $\Delta_\epsilon(t_0) = \sum_i \Delta^i(t_0)\,\epsilon^i$. For small ϵ only the first term is necessary. This is given by

$$\Delta^1(t_0) = \int_{-\infty}^{\infty} \{p_1(x_0(t-t_0), y_0(t-t_0)) \cdot q_0(x_0(t-t_0), y_0(t-t_0)) - q_1(x_0(t-t_0), y_0(t-t_0)) \times p_0(x_0(t-t_0), y_0(t-t_0))\} \exp\left[-\int_0^{t-t_0} \left\{\frac{\partial p_0}{\partial x}(x_0(\xi), y_0(\xi)) + \frac{\partial q_0}{\partial y}(x_0(\xi), y_0(\xi))\right\} \mathrm{d}\xi\right] \mathrm{d}t, \quad (2.13)$$

where $(x_0(t-t_0), y_0(t-t_0))$ denotes the solution of the unperturbed system on Γ_0 starting at $(x_0, y_0) = (x_0(0), y_0(0))$. Arnold (1964) shows how $\Delta^1(t_0)$ can be constructed in another manner in the case of multidimensional Hamiltonian system; see also McGehee & Meyer (1974).

The statement that $\Delta_\epsilon(t_0)$ 'measures the distance between the two branches of the seperatrix of the perturbed system' can be made more precise in terms of the Poincaré map. Consider the cross section of equation (2.10) for some time t_0: $\Sigma_{t_0} = \{x_1, x_2 \mid \theta = \frac{1}{2}\omega t_0/\pi;\ t_0 \in [0, 2\pi/\omega)\}$. If we draw a normal $\boldsymbol{n}$ through some point $(x_0, y_0) \in \Gamma_0 \subset \Sigma_{t_0}$ (cf. figure 3), it will cut M_s^{u} and M_s^{s} at the points $(x_\epsilon^+(t_0, \omega, t_0), y_\epsilon^+(t_0, \omega, t_0))$ and $(x_\epsilon^-(t_0, \omega, t_0), y_\epsilon^-(t_0, \omega, t_0))$ respectively, as Mel'nikov notes. $\Delta_\epsilon(t_0)$ provides a measure related monotonically to the distance $((x_\epsilon^+ - x_\epsilon^-)^2 + (y_\epsilon^+ - y_\epsilon^-)^2)^{\frac{1}{2}}$ for a fixed t_0 (remember that $p_0(x_0, y_0)$ and $q_0(x_0, y_0)$ in (2.12) are fixed). As t_0 varies, the cross section Σ_{t_0} moves and hence the positions of M_s^{u} and M_s^{s} on Σ_{t_0} change; in particular, the points of intersection with $\boldsymbol{n}$, $(x_\epsilon^\pm, y_\epsilon^\pm)$, change. If $\Delta_\epsilon(t_0)$ varies such that it changes sign at some $t_0 = t_0'$ then M_s^{u} and M_s^{s} must intersect near (x_0, y_0) at $\theta' = \frac{1}{2}\omega t_0'/\pi$.

As we point out in the following sections, the existence of homoclinic points at such intersections implies that there is an extremely complex invariant set Ω_{h}, a 'Smale horseshoe', in the neighbourhood of M_s^{s} and M_s^{u}. In particular Ω_{h} possesses orbits of all periods in addition to dense nonperiodic orbits (Chillingworth 1976; Smale 1963, 1965, 1967). We shall be concerned with the effect of Ω_{h} on the global behaviour of orbits of P.

Returning to equation (2.10), we first solve the unperturbed system for the saddle connection Γ_0; i.e. the level curve

$$\tfrac{1}{2}x_2^2 - \tfrac{1}{2}\beta x_1^2 + \tfrac{1}{4}\alpha x_1^4 = 0. \quad (2.14)$$

Recalling that $x_2 = \mathrm{d}x_1/\mathrm{d}t$, we can obtain a relation between x_1 and t by integrating (2.14):

$$t - t_0 = \pm\beta^{-\frac{1}{2}} \int_{x_1(t_0)}^{x_1(t)} \frac{\mathrm{d}x_1}{x_1[1 - (\alpha/2\beta)\,x_1^2]^{\frac{1}{2}}}. \quad (2.15)$$

Writing $(\alpha/2\beta)^{\frac{1}{2}} x_1 = \sin\phi$, integrating (2.15) and taking the initial value $x_1(t_0) = \pm(2\beta/\alpha)^{\frac{1}{2}}$ or $\phi(t_0) = \pm\frac{1}{2}\pi$, we obtain

$$\left.\begin{aligned} &\ln[\tan(\tfrac{1}{2}\phi(t))] = \pm(\beta)^{\frac{1}{2}}(t-t_0), \\ \text{or}\quad &\phi(t) = 2\arctan[\exp(\beta)^{\frac{1}{2}}(t-t_0)] \equiv \operatorname{arc\,cot}(-\sinh((\beta)^{\frac{1}{2}}(t-t_0))). \end{aligned}\right\} \tag{2.16}$$

Thus

$$\left.\begin{aligned} x_1(t) &= (2\beta/\alpha)^{\frac{1}{2}}\operatorname{sech}\tau, \\ x_2(t) &= \beta(2/\alpha)^{\frac{1}{2}}\operatorname{sech}\tau\tanh\tau, \end{aligned}\right\} \tag{2.17}$$

where

$$\tau = \pm\beta^{\frac{1}{2}}(t-t_0).$$

Equations (2.17) are parametric equations for Γ_0 (2.14).

We now insert the appropriate terms $p_1 = 0$, $q_1 = (\bar{f}\cos(\omega t) - \bar{\delta}x_2)$, $p_0 = x_2$, $q_0 = \beta x_1 - \alpha x$ in (2.13) to obtain

$$\begin{aligned} \Delta^1(t_0) &= -\int_{-\infty}^{\infty}(\bar{f}\cos(\omega t) - \bar{\delta}x_2)\,x_2\,\mathrm{d}t, \\ &= \frac{2\delta\beta^2}{\alpha}\int_{-\infty}^{\infty}\operatorname{sech}^2\tau\tanh^2\tau\,\frac{\mathrm{d}\tau}{\beta^{\frac{1}{2}}} - \bar{f}\beta\left(\frac{2}{\alpha}\right)^{\frac{1}{2}}\int_{-\infty}^{\infty}\cos\left[\omega\left(\frac{\tau}{\beta}+t_0\right)\right]\operatorname{sech}\tau\tanh\tau\,\frac{\mathrm{d}\tau}{\beta^{\frac{1}{2}}}, \\ &= \frac{2\delta\beta^{\frac{3}{2}}}{\alpha}\int_{-\infty}^{\infty}\operatorname{sech}^2\tau\tanh^2\tau\,\mathrm{d}\tau - \bar{f}\left(\frac{2\beta}{\alpha}\right)^{\frac{1}{2}}\left[\cos(\omega t_0)\int_{-\infty}^{\infty}\frac{\cos(\omega\tau/\beta)\sinh\tau}{\cosh^2\tau}\,\mathrm{d}\tau\right. \\ &\quad \left. -\sin(\omega t_0)\int_{-\infty}^{\infty}\frac{\sin(\omega\tau/\beta)\sinh\tau}{\cosh^2\tau}\,\mathrm{d}\tau\right]. \end{aligned} \tag{2.18}$$

The second integral in (2.18) is zero, since it is over the product of an odd and an even function. The first integral can be evaluated directly and the third by the method of residues to obtain

$$\Delta^1(t_0) = \tfrac{4}{3}\bar{\delta}\beta^{\frac{3}{2}}/\alpha + \bar{f}\pi\omega(2/\alpha)^{\frac{1}{2}}\operatorname{cosech}(\pi\omega/2\beta^{\frac{1}{2}})\sin(\omega t_0). \tag{2.19}$$

It is clear that for $\bar{\delta} \gg \bar{f}$, $\Delta^1(t_0) > 0$ for all $t_0 \in [0, 2\pi/\omega)$; for small forces, then, we expect to obtain the structure shown in figure 4(*b*). This confirms the invariant manifold results noted above (cf. small perturbation of figure (1)). The critical value of $\bar{f}$, $\bar{f}_c$, for which M_s^u and M_s^s touch, is given by

$$\bar{f}_c \approx \tfrac{4}{3}[\bar{\delta}\beta^{\frac{3}{2}}/\pi\omega(2\alpha)]\sinh(\pi\omega/2\beta^{\frac{1}{2}}). \tag{2.20}$$

Thus, for α, β, $\bar{\delta}$, ω fixed we expect homoclinic motions to occur for $|\bar{f}| > \bar{f}_c$.

Now, recall that $f = \epsilon\bar{f}$, $\delta = \epsilon\bar{\delta}$. For small ϵ, then, we can find the original force amplitude f_c as function of α, β, δ and ω, for which homoclinic motions first appear. We simply drop the overbars in (2.20), and, inserting the values chosen for the analogue computer study in § 3 ($\alpha = 100$, $\beta = 10$, $\delta = 1$, $\omega = 3.76$) we obtain

$$f_c \approx 0.79. \tag{2.21}$$

In view of the symmetry of (2.10) for $\epsilon = 0$ (Γ_0 is a double loop), we expect intersections to occur to the left and right of s simultaneously (cf. § 2.4).

2.4. *Symmetry properties*

Equation (2.4) has the property that, if $(\bar{x}_1, \bar{x}_2, \bar{\theta})$ solves it then so does $(-\bar{x}_1, -\bar{x}_2, \bar{\theta}+\pi/\omega)$. Thus, if an orbit $(\bar{x}_1(t), \bar{x}_2(t))$ exists then it either has a partner $(-\bar{x}_1(t+\pi/\omega), -\bar{x}_2(t+\pi/\omega)$ or it satisfies the symmetry property itself $\bar{x}_1(t) = -\bar{x}_1(t+\pi/\omega)$, $\bar{x}_2(t) = -\bar{x}_2(t+\pi/\omega)$. We call such an orbit *self-similar*.

A number of simple consequences follow from the above:

1. *Subharmonics of period $2\pi N/\omega$ always occur in multiples.* To prove this, suppose that a subharmonic occurs singly and is therefore self-similar. However, self-similarity implies that

$$\bar{x}_j(t) = -\bar{x}_j(t+\pi/\omega) = -(-\bar{x}_j(t+2\pi/\omega)) \equiv \bar{x}_j(t+2\pi/\omega),$$

and that the orbit is therefore in fact harmonic of period $2\pi/\omega$.

2. The period $2\pi/\omega$ saddle orbit $(\bar{x}_1^s(t), \bar{x}_2^s(t))$, whose existence was established in § 2.1, is self-similar.

3. If a homoclinic orbit to $(\bar{x}_1^s(t), \bar{x}_2^s(t))$ exists 'to the right', then a similar homoclinic orbit to $(\bar{x}_1^s(t), \bar{x}_2^s(t))$ exists 'to the left'.

2.5. *A summary of predicted behaviour*

Here we summarize the results obtained in this section relating to the behaviour of solutions of (2.4) as f increases from zero for α, β, δ, ω fixed > 0. For $f = 0$ the straightforward phase portrait of figure 1 applies, and the stable and unstable manifolds M_s^u, M_s^s of the saddle points $= (0, 0)$ retain the structure of the separatrices Γ^u, Γ^s so long as f remains small. Similarly, the three (hyperbolic) fixed points in $\mathbb{R}^2$ of figure 1 become hyperbolic closed orbits in $\mathbb{R}^2 \times S^1$ and the stability types are maintained for small f. Thus we expect the averaging theorem applied locally near $(x_1, x_2) = (\pm(\beta/\alpha)^{\frac{1}{2}}, 0)$ to give reasonable results (equation (2.9) with ρ replaced by $\nu = 2\beta - \omega^2$).

As f continues to increase, M_s^u and M_s^s begin to wind back and forth, and ultimately, for $f \approx f_c$, they touch. They then intersect transversally for all $f > f_c$, giving rise to homoclinic motions. f_c is given by equation (2.20). We do not yet know how the homoclinic intersections affect the attracting closed orbits 'near' $(\pm(\beta/\alpha)^{\frac{1}{2}}, 0)$, but, in view of (2.5), we do know that global attraction is preserved.

Finally, for f large, we expect the averaging theorem to yield reasonable results again, since forced motions will occur which lead to orbits surrounding the positions of all three fixed points of figure 1.

In the remainder of this paper we make use of analogue computer results and of constructions of the Poincaré map to study the bifurcations of (2.4) occurring for $f \geqslant f_c$.

3. Analogue computer studies of the o.d.e.

3.1. *General behaviour: the Poincaré map*

Using the analogue computer to solve (2.4) and recording only the peak amplitude of $x = x_1(t)$ for various fixed values of f, β, δ, α, ω, we obtain the data shown on figure 5. We also show the response curves predicted from the averaging analysis of § 2.2. It is clear that for $f \lesssim 0.5$ and $f \gtrsim 2.5$ the averaged results are reasonable. However, for $f \in (1.08, 2.45)$ they fail completely. In this region, indicated by the shaded box, solutions behave in a complex and erratic manner. A typical solution trajectory, projected down from (x_1, x_2, θ) space to (x_1, x_2) space, is shown in figure 6. The apparent crossing and branching of solution curves is an artefact of the projection (cf. Cook & Roberts (1970), figs 3–4, where solutions of an autonomous system with a strange attractor are shown). Note that figure 6 represents the situation many minutes after computation commenced and that all the transient behaviour

PHILOSOPHICAL TRANSACTIONS OF THE ROYAL SOCIETY A MATHEMATICAL, PHYSICAL & ENGINEERING SCIENCES

had decayed to insignificant proportions. Thus we shall assume that figure 6 represents a sample of the type of solution found in the attracting set $S \in A$ for the parameter values indicated.

At first sight figure 6 appears extremely complicated. However, if instead of examining solution curves of the o.d.e. we examine successive iterates of the Poincaré map, P: $\mathbb{R}^2 \to \mathbb{R}^2$; $\mathbb{R}^2 = \{x_1, x_2 | \theta = 0, 2\pi/\omega, 4\pi/\omega, \ldots\}$, the behaviour is considerably clearer. Using a track-hold device, the computer records the values of x_1 and x_2 at the appropriate times and feeds these values to a plotter. The techniques are quite well known and have been used by various workers; cf. Tondl (1976), Fiala (1975) and Hayashi *et al.* (1969, 1970, 1973). Hayashi has obtained some results similar to those below. Typical results are shown in figure 7. In figure 7*a* ($f = 0.2$) the structure of stable and unstable manifolds is simple and qualitatively identical to that of the damped oscillator with no external force, equation (2.4), figure 1. The local presistence of closed orbits (fixed points of the Poincaré map) is clear throughout figures 7*a–d*. However, as f increases, the *global* behaviour of the manifolds of saddle point s becomes increasingly complicated until, at $f = f_c \approx 0.76$, the stable and unstable manifolds M_s^s and M_s^u

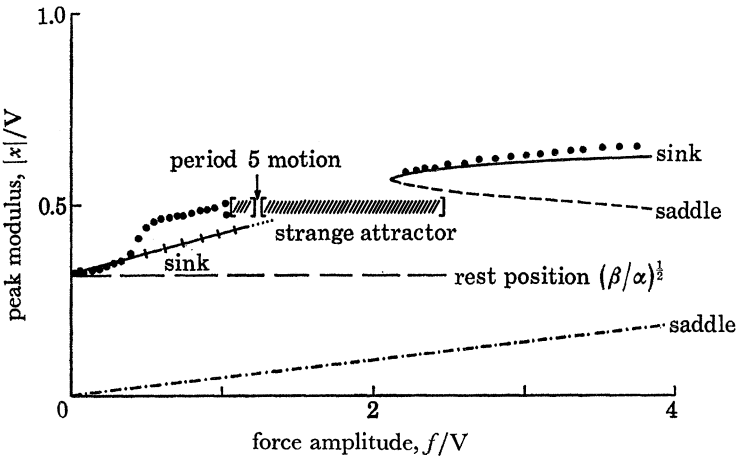

FIGURE 5. Analogue computer measurements of response amplitude versus force: $\alpha = 100$, $\beta = 10$, $\delta = 1$, $\omega = 3.76$. For $f < 1$ and $f > 2$, where periodic almost sinusoidal response is obtained, the experimental measurements indicate the peak modulus of an equivalent (equal power) sine wave. In the region $f \in (1.1, 2.5)$ non-periodic motions are observed, these are denoted by hatching and are marked 'strange attractor'. At $f \approx 0.95$ the periodic orbits bifurcate to orbits of period 2 and in an open interval $f \in (1.15, 1.2)$ a period 5 motion is observed in place of the strange attractor. ——, – –, –·–, equation (2.9), $\rho = -\beta - \omega^2$; ++, equation (2.9) $\nu = 2\beta - \omega^2$; ....., measurement-peak modulus of equivalent sine wave.

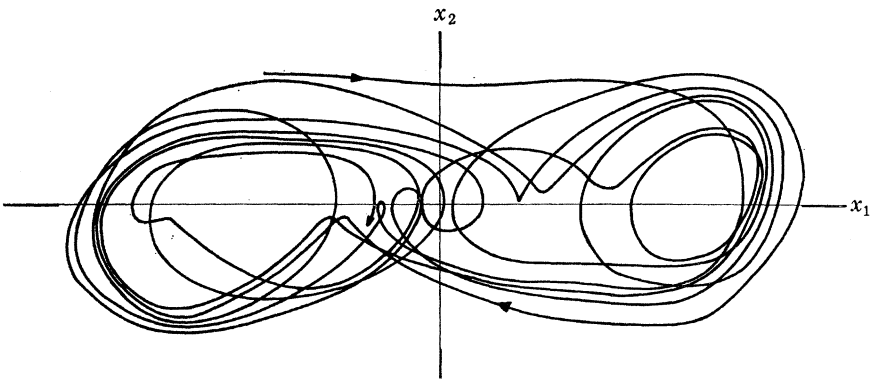

FIGURE 6. Solution curves projected on to (x_1, x_2) space for $f = 1.5$, $\alpha = 100$, $\beta = 10$, $\delta = 1$, $\omega = 3.76$.

touch and then, for $f \gtrsim 0.76$, intersect transversally. Intersections of left-hand manifolds M^{u}_{sl}, M^{s}_{sl} and right hand manifolds M^{u}_{sr}, M^{s}_{sr} occur simultaneously: see § 2.4. The strong contraction and expansion associated with P forces almost all of these intersections to occur in a narrow strip close to the location of Γ_0 (figure 3) and only a few intersections are shown in figures 7*c* and *d*.

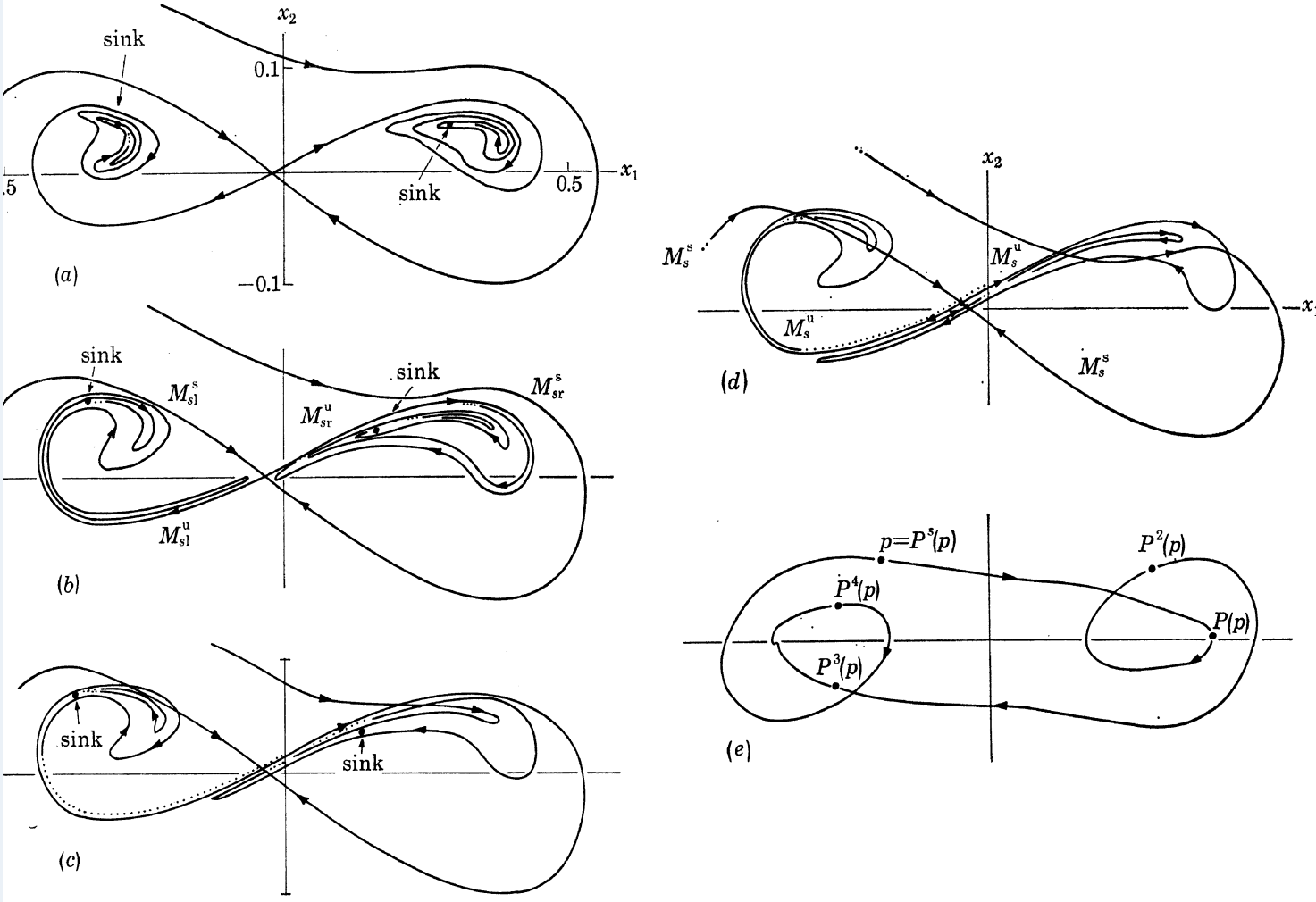

FIGURE 7. Analogue computer plots of the Poincaré map: stable and unstable manifolds of s for various force levels: $\alpha = 100$, $\beta = 10$, $\delta = 1$, $\omega = 3.76$; (*a*) $f = 0.2$; (*b*) $f = 0.75$; (*c*) $f = 0.90$; (*d*) $f = 1.10$; 'strange attractor': successive iterates approach and tend to remain on M^{u}_{s}; (*e*) $f = 1.20$: Period 5 motion.

The parameter value at which M^{s}_{s} and M^{u}_{s} first touch $\{f_c \approx 0.76 | \delta = 1, \beta = 10, \alpha = 100, \omega = 3.76\}$ compares very well with the value of $f_c \approx 0.79$ predicted by the method of Mel'nikov in § 2.3. According to the theory, for $f > f_c$ transversal homoclinic intersections persist (cf. Morosov 1976, § 4). Physically the presence of homoclinic motions causes solutions of the o.d.e. (and hence iterates of P) to 'wander' in an apparantly irregular manner for some time before approaching an attracting set.

Note that for $f = 0.9$ (figure 7*c*) the sinks of P still exist and almost all orbits of P approach either one of these as $t \to +\infty$. These fixed points remain sinks until $f \approx 0.95$, at which value they become saddle points, each throwing off a pair of sinks and thus creating two orbits of period 2. The bifurcation therefore appears to involve one simple eigenvalue of $DP(a^{\pm})$, the

map P linearized at either sink ($a^{\pm}$), passing through -1 while the other is negative and of modulus < 1. The discussion of § 2.4 shows that these bifurcations occur simultaneously.

At $f \approx 1.04$ a second bifurcation occurs in which the orbits of period 2 become unstable and throw off orbits of period 4. A sequence of successive bifurcations to periods 8, 16, 32 then appears to occur, with an accumulation point at $f \approx 1.08$. After the period 8 motions the periodic points in P can no longer be clearly distinguished. For $f \gtrsim 1.08$ successive iterates of P move in an irregular fashion in the sense that they do not seem to be attracted to a periodic point. Power spectra taken from up to 10^4 iterates indicate no periodic behaviour (see § 3.2). However, attracting points of very high period may be present and the rate of attraction may be low. Computational results merely suggest that for $1.08 \lesssim f \lesssim 2.45$ a 'strange attractor' exists. Henceforth we call this attractor S; in the remainder of this paper we shall be concerned with a study of its structure. But first, we note one further feature which suggests the presence of a strange or chaotic motion. For certain parameter ranges stable attracting motions of period 5 appear in place of the strange motion; power spectra indicate that these are genuine, persistent phenomena. A typical motion is shown in figure 7*e*, with the periodic points of P indicated. We consider the implications of this in § 4, below.

3.2. *The structure of attracting set S for* $f \in (1.08, 2.45)$

Although we study a specific attracting set arising in a particular o.d.e. in this paper, both the attractor and motions occurring in its neighbourhood appear to share many features in common with other strange attractors (Hénon 1976; Lorenz 1963; Guckenheimer 1976). This study should therefore be of general interest.

One feature immediately apparent in analogue computer studies (figure 7*d*) is that orbits of P appear to approach the unstable manifold M_s^u of s, just as for $f \lesssim 1.08$. However, instead of approaching an attractor either to the right or left of s, as for $f \lesssim 1.08$, successive iterates of P merely continue to approach M_s^u and, since M_s^u intersects M_s^s and winds about in a complex manner, the orbits must follow this behaviour. Observations indicate that orbits continue to cross between right and left half-planes for at least 10^6 iterates. For $f \gtrsim 1.08$ the distinct periodic attractors originally lying in the right and left half-planes apparently no longer exist and we are led to postulate the existence of (at least one) attracting set S intersecting *both* half planes. Presumably iterates of P tend to approach S along or close to M_s^u.

If we assume that, ignoring the first hundred iterates of P, almost all orbits have approached arbitrarily closely† to S, then it is the structure of S that is actually displayed in figure 7*d*. It appears to be the product of a curve and a Cantor set. This is identical to the structure proposed by Hénon (1976) on the basis of digital computer work on a two dimensional map. Hénon's conclusion has been questioned (Newhouse 1977; Zeeman, E. C., personal communication), and it has been suggested that the motion he observed may have been merely in the neighbourhood of a Smale horseshoe (Smale 1967) arising from the homoclinic intersections, and that iterates would eventually approach a periodic orbit of very high period (see § 5.3, below). However, the number of iterates examined by Hénon (5×10^6) and the present results strongly suggest that a genuine non-periodic strange attractor is present in this and related systems. We consider this in more detail in §§ 4 and 5 below. For the moment note that the

† The rate of convergence is very rapid. After 3 or 4 iterates of an arbitrarily chosen point p the distance between $P^4(p)$ and M_s^u is generally undetectable. For $f \lesssim 1.08$ only 10 or 15 iterates are necessary for orbits to approach to within an undetectable distance of a sink or periodic point.

PHILOSOPHICAL TRANSACTIONS OF THE ROYAL SOCIETY A MATHEMATICAL, PHYSICAL & ENGINEERING SCIENCES

structure of S appears to be closely related to the existence of homoclinic points in P and that the absence of short period attractors for $f \gtrsim 1.08$ and the presence of globally stabilizing nonlinear terms (§ 2.1) ensures that orbits behave in a complicated manner but that they approach, enter and remain within a closed set containing S as $t \to +\infty$.

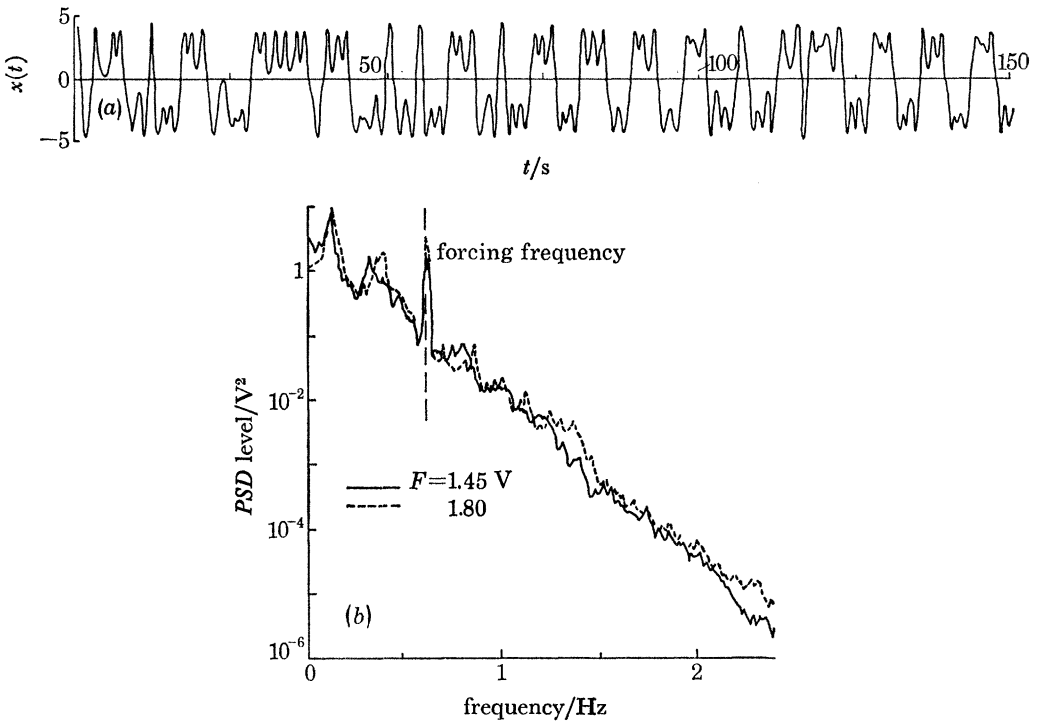

FIGURE 8. Time series and power spectra of the nonlinear oscillator: $\delta = 0.2$, $\beta = 10$, $\alpha = 100$, $\omega = 0.6$ Hz ≈ 3.76 rad/s. (*a*) Typical time series of $x(t)$ after decay of starting transients, $f = 1.80$; (*b*) Power spectra for two force levels. Resolution = 0.01 Hz; 74 degrees of freedom.

Part of a typical time history $x_1(t)$ is shown in figure 8*a*, in which two time scales are apparent, associated with the erratic changes in sign and with the oscillations approximately at the forcing frequency. Since $x(t)$ has a 'random' appearance, it is natural to investigate the statistical properties of $x(t)$, and in particular the power spectrum and autocorrelation function.

3.3. *Power spectra of motions in S: summary of behaviour*

In figure 8*b* we show two power spectra for different force levels f (the damping parameter, δ, differs from that used in figures 7*a–d*: this was merely a matter of convenience and resulted in no qualitative changes in behaviour). Note that the spectra are essentially continuous and ln (*PSD*) falls in an almost linear manner with frequency, indicating a law of the form $X(\omega) \approx A\,\mathrm{e}^{-b\omega}$. Some periodic behaviour at the forcing frequency is apparent but the response spectrum is not untypical of a broad-band random process, although *it arises from a deterministic o.d.e.* Correlation function measurements provide further confirmation of this. The high level of the spectrum at low frequencies is evidently due to the longer time scale associated with changes in sign occurring in $x(t)$ when the orbit of P moves from left to right half-plane and vice versa. In a physical system the frequency of and conditions under which such changes occur would clearly be of great interest.

Before considering a theoretical model for P we first summarize the qualitative features detected by computer and theoretical studies of the o.d.e.

(i) P is globally stable in the sense that all orbits approach and enter some closed set $A \subset R^2$ as $t \to +\infty$.

(ii) P has a natural symmetry inherited from the invariance of the o.d.e. to transformations of the form $(x_1, x_2, t) \to (-x_1, -x_2, t+\pi/\omega)$.

(iii) As f changes the following phenomena are present in P: (*a*) $0 \leqslant f \lesssim 0.4$: two sinks $a^{\pm}$ with complex conjugate eigenvalues and one saddle with positive eigenvalues. The saddle persists unchanged for all f. (*b*) $0.5 \lesssim f \lesssim 0.76$: the sinks $a^{\pm}$ now have real, negative eigenvalues. Locally, near a^+ and a^-, the map therefore induces a rotation through π. (*c*) $0.76 \lesssim f \lesssim 0.95$: homoclinic points appear and persist for all $f \gtrsim 0.76$. (*d*) $0.95 \lesssim f \lesssim 1.04$: the sinks bifurcate at $f_1 \approx 0.95$, becoming saddles and throwing off points of period 2. (*e*) $1.04 \lesssim f \lesssim 1.08$: A sequence of bifurcations occur at $f_2, f_3, \ldots$ in which points of periods 4, 8, 16, 32, ... appear. At $f_1 \approx 1.08$ a motion of very high period *or* a 'strange attractor' S appears. f_1 appears to be an accumulation point of the sequence $f_1, f_2, \ldots$. (*f*) $1.08 \lesssim f \lesssim 2.45$: S exists and attracts nearby solutions. Finally, for $f \gtrsim 2.15$ an additional pair of fixed points, a sink and a saddle, appear 'outside' the homoclinic points and S. After each of the bifurcations at the f_i, $i = 1, 2, 3, \ldots$ for $f_i \in (0.95, 1.08)$ the newly created saddle points remain for all $f > f_i$. Thus for $f \gtrsim 1.08$ we apparently have an infinite number of saddles of periods 2, 4, 8, 16, ..., etc., associated with the original sinks and also a countable infinity of periodic points due to the homoclinic intersections of M_s^u and M_s^s (Chillingworth 1976; Smale 1965).

4. Approximating the Poincaré map

In this section we develop an approximate representation, P_d, of the Poincaré map P of (2.4) as a difference equation on $\mathbb{R}^2$. Since (2.4) cannot be solved explicitly we solve the linear system obtained by setting $\alpha \equiv 0$ and take the resulting linear map as the linear part of P_d. We then choose the simplest nonlinear function with the required qualitative properties and add this to complete P_d. Although this may seem naïve, we shall see that P_d reproduces the behaviour of P remarkably well.

4.1. *The o.d.e. as an integral equation*

We first apply a standard linear transformation to put equation (2.4) into a more convenient form:

$$\left.\begin{aligned} \dot{u} &= \lambda^+ u - [\alpha'(u+v)^3 - f' \cos\theta], \\ \dot{v} &= \lambda^- v + [\alpha'(u+v)^3 - f' \cos\theta], \\ \dot{\theta} &= \omega, \end{aligned}\right\} \tag{4.1}$$

where $\lambda^{\pm} = -\frac{1}{2}\delta \pm \sqrt{(\beta + \frac{1}{4}\delta^2)}$, $\alpha' = \alpha/\sqrt{(\beta+\frac{1}{4}\delta^2)}$ and $f' = f/\sqrt{(\beta+\frac{1}{4}\delta^2)}$.

Here λ^+ and λ^- are the eigenvalues of the *autonomous* o.d.e. (2.1) linearized at the saddle point $(0, 0)$. For specific initial conditions (u_0, v_0, θ_0) (4.1) can be rewritten as an integral equation

$$\left.\begin{aligned} u(t) &= u_0 e^{\lambda^+ t} - \int_0^t e^{\lambda^+(t-\tau)} \{\alpha'(u(\tau)+v(\tau))^3 - f' \cos(\theta_0 + \omega\tau)\}\, d\tau, \\ v(t) &= v_0 e^{\lambda^- t} + \int_0^t e^{\lambda^-(t-\tau)} \{\alpha'(u(\tau)+v(\tau))^3 - f' \cos(\theta_0 + \omega\tau)\}\, d\tau. \end{aligned}\right\} \tag{4.2}$$

To obtain an expression for the Poincaré map P we set $\theta_0 = 0$ and $t = 2\pi/\omega$; (4.2) then yields a difference equation relating successive iterates of P. The linear and externally forced terms can be evaluated directly to give

$$\left.\begin{aligned} u_{i+1} &= \gamma^{\mathrm{u}} u_i + f'\lambda^{+}(\gamma^{\mathrm{u}}-1)/(\lambda^{+2}+\omega^2) - \gamma^{\mathrm{u}}\alpha' g_1(u_i, v_i), \\ v_{i+1} &= \gamma^{\mathrm{s}} v_i - f'\lambda^{-}(\gamma^{\mathrm{s}}-1)/(\gamma^{-2}+\omega^2) + \gamma^{\mathrm{s}}\alpha' g_2(u_i, v_i). \end{aligned}\right\} \tag{4.3}$$

Here $\gamma^{\mathrm{u}} = \mathrm{e}^{2\pi\lambda^{+}/\omega}$ and $\gamma^{\mathrm{s}} = \mathrm{e}^{2\pi\lambda^{-}/\omega}$ are the eigenvalues of $DP_0(0, 0)$, the Poincaré map *of the unforced system* linearized at the saddle. The nonlinear terms

$$g_1 = \int_0^{2\pi/\omega} \mathrm{e}^{-\lambda^{+}\tau}(u(\tau)+v(\tau))^3\,\mathrm{d}\tau \quad \text{and} \quad g_2 = \int_0^{2\pi/\omega} \mathrm{e}^{-\lambda^{-}\tau}(u(\tau)+v(\tau))^3\,\mathrm{d}\tau$$

cannot be evaluated explicitly.

We now apply a second transformation to put the Poincaré map back in terms of the original displacement and velocity coordinates $(x, y) \equiv (x, \dot{x})$. Using $\begin{Bmatrix} x \\ y \end{Bmatrix} = T \begin{Bmatrix} u \\ v \end{Bmatrix}$, where $T = \begin{bmatrix} 1 & 1 \\ \gamma^{\mathrm{u}} & \gamma^{\mathrm{s}} \end{bmatrix}$, we obtain

$$\left.\begin{aligned} x_{i+1} &= y_i + f'\{\lambda^{+}(\gamma^{\mathrm{u}}-1)/(\lambda^{+2}+\omega^2) - \lambda^{-}(\gamma^{\mathrm{s}}-1)/(\lambda^{-2}+\omega^2)\} + g_1'(x_i, y_i), \\ y_{i+1} &= -\gamma^{\mathrm{u}}\gamma^{\mathrm{s}} x_i + (\gamma^{\mathrm{u}}+\gamma^{\mathrm{s}})\, y_i + f'\{\gamma^{\mathrm{u}}\lambda^{+}(\gamma^{\mathrm{u}}-1)/(\lambda^{+2}+\omega^2) \\ &\qquad - \gamma^{\mathrm{s}}\lambda^{-}(\lambda^{\mathrm{s}}-1)/(\lambda^{-2}+\omega^2)\} + g_2'(x_i, y_i), \end{aligned}\right\} \tag{4.4}$$

where g_1' and g_2' are defined in the obvious way. We can make a further change of coordinates such that the saddle point of P is shifted to the origin (the invariant manifold theorem and the work of § 3 ensures that P *has* a saddle for $f \neq 0$ as well as for $f = 0$; for small f, in fact, we expect the eigenvalues of s to be close to γ^{u} and γ^{s} of the unperturbed system). In the remainder of this section then, we shall study difference equations of the form

$$\left.\begin{aligned} x_{i+1} &= y_i + F(x_i, y_i), \\ y_{i+1} &= -bx_i + dy_i + G(x_i, y_i); \quad b,\, d > 0. \end{aligned}\right\} \tag{4.5}$$

where $b \approx \gamma^{\mathrm{u}}\gamma^{\mathrm{s}}$ and $d \approx (\gamma^{\mathrm{u}}+\gamma^{\mathrm{s}})$. There would also generally be a (small) term ϵx_i in the first equation, but we drop this for simplicity: it is certainly possible to find a change of coordinates that will remove it. The important point to note is that (4.5) has a saddle point with eigenvalues $|\gamma_d^{\mathrm{u}}| > 1$, $|\gamma_d^{\mathrm{s}}| < 1$, γ_d^{u} and $\gamma_d^{\mathrm{s}} > 0$ and $|\gamma_d^{\mathrm{u}}\gamma_d^{\mathrm{s}}| < 1$ if b and d are chosen appropriately. For small f, γ_d^{u} and γ_d^{s} are close to γ^{u} and γ^{s} defined above. The local qualitative properties of P_d, the approximate Poincaré map given by (4.5), are then identical to those of the o.d.e's Poincaré map P studied above and in § 3. For the studies below we take $b = 0.2$ and $d \in (2, 2.8)$; the reader can check that the eigenvalue conditions specified above are satisfied. Note that the linear terms in (4.5) take a standard form which is closely related to the local coordinate systems employed by Gavrilov & Silnikov (1972, 1973) in studies of homoclinic motions.

Having fixed the linear part of our approximate map P_d, we now consider the nonlinear terms F and G. Since explicit expressions cannot be obtained we resort to a subterfuge. We choose to study the 'simplest' nonlinear difference equation with the requisite properties outlined at the end of § 3 (cf. Hénon 1976). We shall study an analytic one-to-one map; note that the Poincaré map actually may not be analytic, but the existence and uniqueness theorem for o.d.es guarantees that a Poincaré map *can* be defined and that it will be one to one and possess some differentiability (here, in fact, it will be C^{∞}).

4.2. *The 'simplest' cubic map*

The studies of §§ 2 and 3 indicate that homoclinic motions are of great importance in S. We therefore consider the maps introduced by Smale (1963, 1965, 1967) in this connection. The classical Smale horseshoe (cf. [3]) is a one to one map f which takes a square in $\mathbb{R}^2$, simultaneously stretches and bends it and replaces it over itself as indicated in figure 9*a*. Here, however, we have (qualitative) symmetry about the central saddle $(0, 0) \in \mathbb{R}^2$ and we therefore study an alternative map with similar properties (Smale 1967), figure 9*b*. In particular, we are interested in one parameter maps with a parameter related to f of (2.4) which, for small f, possess a saddle and two sinks. As f increases homoclinic interactions should occur and the sinks should undergo the sequence of bifurcations outlined at the end of § 3. Ideally the global stability properties should also be preserved.

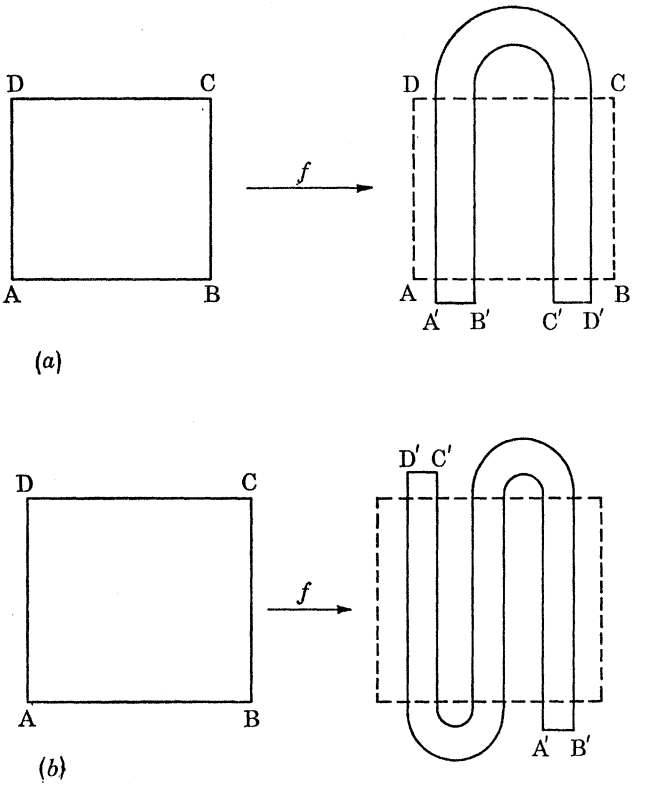

FIGURE 9. Two maps related to homoclinic motions. (*a*) The Smale horseshoe; (*b*) a double horseshoe.

The quadratic map studied by Hénon (1976) corresponds closely to the classical horseshoe of figure 9*a*. It can be written in the form

$$\left.\begin{aligned} x_{i+1} &= by_i, \\ y_{i+1} &= x_i - ky_i - ay_i^2; \quad k = (1-b) - [(1-b)^2 + 4a]^{\frac{1}{2}}, \end{aligned}\right\} \tag{4.6}$$

and possesses a saddle point at (0, 0) and a second fixed point at $((b-k-1), b(b-k-1))$. For b fixed ≈ 0.3 and a 'small', this second point is a sink. As a increases it undergoes the sequence of bifurcations to periods 2, 4, 8, 16, ... described in § 3. Ultimately an apparently non-periodic strange attractor appears. Furthermore, Hénon shows that maps of the form (4.6)

are representative of the most general quadratic mappings with constant Jacobian. Here, to satisfy the symmetry requirement, we are therefore naturally led to consider an analogous cubic map. We preserve the linear component derived in (4.5) and study the map P_d given by

$$\left.\begin{aligned} x_{i+1} &= y_i, \\ y_{i+1} &= -bx_i + dy_i - y_i^3. \end{aligned}\right\} \tag{4.7}$$

As we show below this provides an analogue of the map of figure 9*b*.

For small force f we know that $b \approx \gamma^u\gamma^s$ and $d \approx \gamma^u + \gamma^s$, where $\gamma^u = e^{2\pi\lambda^+/\omega}$ and $\gamma^s = e^{2\pi\lambda^-/\gamma}$, the eigenvalues of the true linearized Poincaré map for $f = 0$. Inserting values for the o.d.e. studied in § 3 ($\beta = 10$, $\delta = 1$, $\omega = 100$, $\omega = 3.76$) we obtain $b \approx 0.19$, $d \approx 93$. The rate of expansion is thus extremely high and it is this that makes the details in figure 7 so difficult to interpret. Since we are primarily interested in the qualitative structure of S, we reduce d considerably in our numerical studies below. Moreover, exploratory computations showed that nothing is gained by adding a variable coefficient to the cubic term of (4.7) and we therefore fix b and merely vary d to reproduce the action of varying f in the o.d.e.

We note an important inadequacy of the map (4.7): it is not globally attracting, since for large y_i orbits clearly escape to infinity as $i \to \infty$. However, a 'trapping region' $D \subset \mathbb{R}^2$ can easily be defined such that all orbits starting in D remain in D as $t \to +\infty$ and in fact approach one of the attractors or saddles in D; cf. (Hénon 1976). To make (4.7) globally attracting we would merely have to modify the nonlinear term suitably: it is easy to devise non-analytic maps with the required properties, but here, for simplicity, we shall ignore this feature of P_d. We shall see in § 5 that P_d preserves almost all the other significant features of P noted in § 3.

4.3. *Properties of some maps on the unit interval and on the square*

Before studying P_d in detail we consider some more general points. First we consider one dimensional analogues of the maps with properties of interest to us. The quadratic map

$$x_{i+1} = ax_i - x_i^2, \tag{4.8}$$

and similar maps have received much attention (Hsu *et al.* 1975; Li & Yorke 1975; Lorenz 1964; May 1974). Here, to satisfy symmetry requirements, we would naturally study

$$x_{i+1} = ax_i - x_i^3. \tag{4.9}$$

The properties of such maps are somewhat understood. First note that they are *not* one to one whereas the planar maps (4.6) and (4.7) are; they are globally attracting, however, if we take a suitable intervals $I \subset \mathbb{R}$, both (4.8) and (4.9) map I into itself.

Now consider what happens as the parameter a increases in (4.9). For $a < 1$ there is a single sink at 0; at $a = 1$ this becomes a source and two further fixed points appear at $\bar{x} = \pm\sqrt{(a-2)}$. For $a \in (1, 2)$ these are sinks and then at $a = 2$ each bifurcates to create periodic points of period 2. A sequence of bifurcations to points of period 4, 8, 16, ... then occurs. Presumably an accumulation point a_1 exists at which a non-periodic motion or 'chaos' appears. This is known to occur for (4.8). The sequence of bifurcations is well understood and an important theorem on the structure of sets of periodic points of such one dimensional maps was proved by Šarkovskii (1964) (cf. Stefan 1977) and later reproved by Li & Yorke (1975). Basically there is an order relation on the set N of all integers $\geqslant 1$. First let $N = A \cup B$ and let

$A = \{2^n l \mid n \geqslant 0, l \geqslant 3, l \text{ odd}\}$, $B = \{2^m \mid m \geqslant 0\}$. Order A with increasing n and l and order B with decreasing m; let A precede B we then obtain an ordered sequence of the form

$$3 \blacktriangleleft 5 \blacktriangleleft 7 \blacktriangleleft \ldots \blacktriangleleft 2.3 \blacktriangleleft 2.5 \blacktriangleleft \ldots \blacktriangleleft 4.3 \blacktriangleleft 4.5 \blacktriangleleft \ldots \blacktriangleleft 8.3 \blacktriangleleft \ldots \blacktriangleleft 16 \blacktriangleleft 8 \blacktriangleleft 4 \blacktriangleleft 2 \blacktriangleleft 1. \quad (4.10)$$

The theorem of Šarkovskii may then be stated:

THEOREM. *Let $P: \mathbb{R} \to \mathbb{R}$ be a continuous map with a periodic orbit of period n. Then P has a periodic orbit with period m for every $m \in N$ such that $n \blacktriangleleft m$.*

Thus period 16 implies periods 8, 4, 2 and 1 (a fixed point) and period 3 implies *everything* else, or chaos (Li & Yorke 1975). It is clear that as the sequence of bifurcations noted above occurs, orbits of arbitrarily high period appear (2^n; $2^n l$; $n \to \infty$). See Lorenz (1964) for a general discussion of such phenomena. Lorenz also discusses the use of statistical measures in the study of maps such as (4.8) and (4.9). Li & Yorke carry this further and prove that an invariant measure exists for such maps. The ergodic mixing property of maps such as (4.8) and (4.9) is closely related to their geometric property of folding the interval I (once in the case of (4.8) and twice in (4.9)) and replacing the folded interval within itself.

The one dimensional studies are relevant to our two dimensional map in the following way. With a suitable (nonlinear) charge of coordinates $(x, y) \to (u, v)$, maps such as P_d can sometimes be put into the form $(u, v) \to (f(u), g(u, v))$, where $f(u)$ is itself of the form $u_{i+1} = au_i - u_i^3$ and $g(u, v)$ provides a contraction in a direction transverse to u. As $i \to +\infty$, then, all orbits approach the u axis and the component $f(u) = au - u^3$ essentially captures much of the behaviour *but not the homoclinic structure*, for which a two dimensional map is necessary. However, as we shall see, the sequence of bifurcations of (4.8)–(4.9) occurs for P_d and Šarkovskii's theorem also seems to apply. For examples of the use of a one dimensional map in the analysis of a three dimensional flow, see Guckenheimer (1978), Rand (1978) and Williams's (1978) work on the Lorenz equations.

5. Digital computer studies of the map P_d

5.1. *Fixed points and bifurcations*

We first establish some basic properties of the map P_d:

$$\left.\begin{aligned} x_{i+1} &= y_i, \\ y_{i+1} &= -bx_i + dy_i - y_i^3; \quad d \geqslant 0, b > 0. \end{aligned}\right\} \quad (5.1)$$

We regard d as the parameter. P_d has a fixed point at $(0, 0)$ for all d; for $d < 1+b$ this is a sink and for $d > 1+b$ a saddle with two positive eigenvalues. At $d = 1+b$ two new fixed points appear at $(\pm(d-b-1)^{\frac{1}{2}}, \pm(d-b-1)^{\frac{1}{2}})$; these are sinks for $d < 2(1+b)$ and for $d > 2(1+b)$: saddles with two negative eigenvalues, one of modulus > 1. At $d = 2(1+b)$ bifurcations to orbits of period 2 thus occur. As d continues to increase a sequence of bifurcations occurs exactly as in the one dimensional maps (4.8–9). After each bifurcation the saddles thus created (of periods 1, 2, 4, 8, ...) persist unchanged on d increases. As we shall see below, for $d \approx 2.3(1+b)$ non-periodic motions or motions of very high period appear, just as Šarkovskii's theorem suggests. For approximations to the true Poincaré map of the strange attractor S, we are therefore interested in studying the behaviour of (5.1) for $d \in (1+b, 2.4(1+b))$.

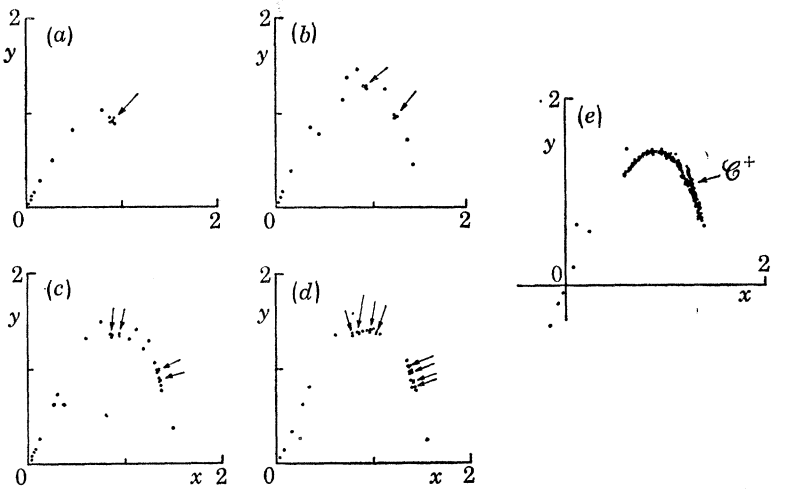

FIGURE 10. Successive iterates of P_d, $b = 0.2$, initial conditions $(x_0, y_0) = (0.0001, 0.0001)$. (*a*) $d = 2.0$: period 1; (*b*) $d = 2.5$: period 2; (*c*) $d = 2.65$: period 4; (*d*) $d = 2.662$: period 8; (*e*) $d = 2.71$: nonperiodic motion.

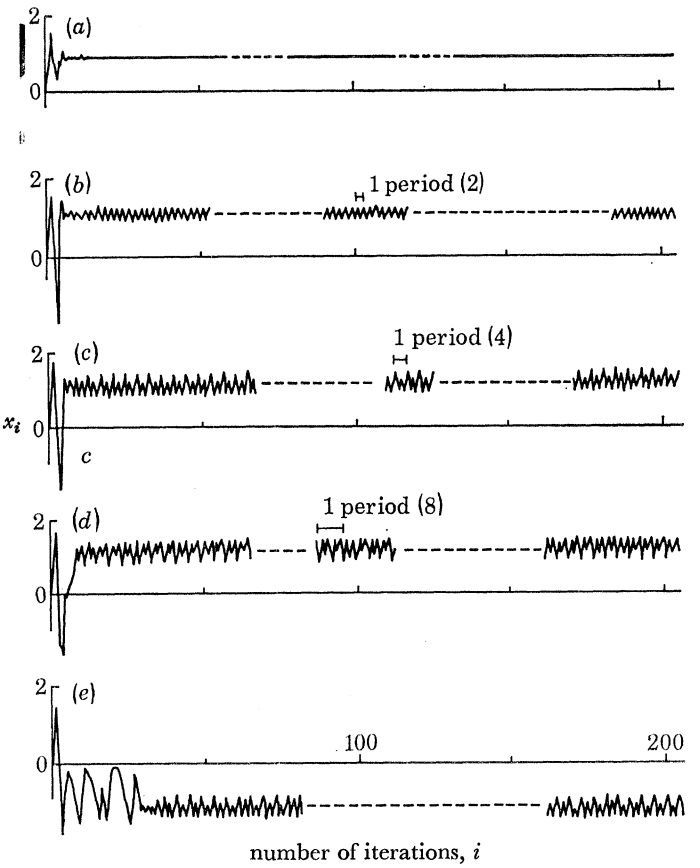

FIGURE 11. Time series of P_d; $b = 0.2$, initial conditions $(x_0, y_0) = (0.0001, 0.0001)$ except in case (*e*). (*a*) $d = 2.0$; (*b*) $d = 2.5$; (*c*) $d = 2.65$; (*d*) $d = 2.662$; (*e*) $d = 2.662$; initial conditions (0.0001, 0.0003).

5.2. *Computer studies: the global behaviour of* P_d

For digital studies we fix $b = 0.2$ and vary d. The sequence of bifurcations of fixed points noted above is illustrated in figure 10, where points of period 1, 2, 4 and 8 are shown for $d = 2$, 2.5, 2.65 and 2.662. The evolutions of x_i, $i = 1, 2, 3, \ldots$ are shown in figure 11. In each case an initial condition of $x_0, y_0 = (0.0001, 0.0001)$ was taken. This is close to the unstable manifold of the saddle at (0, 0). Successive bifurcations are increasingly difficult to detect but can be followed at least up to period 32. In all cases a second (set of) fixed point(s) exists in the $(-x, -y)$ quadrant.

Successive bifurcations occur at closer and closer intervals as d continues to increase until at $d \approx 2.70$ an apparently non-periodic attracting motion appears (figure 10*e*). The orbits appear to be restricted to two distinct (sets of) curves in the (x, y) or $(-x, -y)$ quadrants respectively. Repeated application of the local (eigenvalue) analysis sketched in § 5.1 strongly suggests that all the periodic points retain one dimensional stable manifolds (one eigenvalue with modulus < 1) and that we therefore have two 'expanding attractors', each with infinitely many periodic points lying on some curves $\mathscr{C}^{\pm}$ in $\mathbb{R}^2$, (figure 10*e*). P_d apparently maps $\mathscr{C}^+(\mathscr{C}^-)$ into itself. Neglecting the attracting direction transverse to $\mathscr{C}^{\pm}$ the behaviour of the attractor seems identical to that observed in the one dimensional maps (4.8–9), with the sequence of periodic orbits appearing as Šarkovskii's theorem suggests. A further increase in d results (at $d \approx 2.75$) in the two distinct attractors becoming interlaced so that successive iterates of P_d are continually thrown back and forth between the (x, y) and $(-x, -y)$ quadrants. To understand this we must consider the global behaviour of P_d.

To study global behaviour we establish the structure of the stable and unstable manifolds M^{s}_d and M^{u}_d of the saddle point at (0, 0) by taking a small rectangle $\mathscr{R} = \{x, y \mid |x| \leqslant 10^{-3}, |y| \leqslant 10^{-3}\}$ and iterating $P_d(\mathscr{R})$ forwards p times and backwards q times. The boundary of $\mathscr{R}$ under P^p_d and P^{-q}_d then approximates very closely those parts of M^{u}_d and M^{s}_d 'closest' to (0, 0). In figure 12*a*, for $d = 2.5$ ($p = 12$, $q = 5$) the stable and unstable manifolds have not yet intersected. M^{s}_d and M^{u}_d touch for $d \approx 2.60$ and at $d = 2.65$ the transversal (homoclinic) intersections are clear (figure 12*b*). The structure of M^{s}_d and M^{u}_d for $d \gtrsim 2.60$ suggests that, depending on initial conditions, successive iterates of P_d might be carried back and forth for some time before finally approaching an attracting orbit. Figures 11*d*, *e* bear this out; the initial conditions here were (0.0001, 0.0001) and (0.0001, 0.0003) respectively. Note that the two orbits approach different attractors as $i \to \infty$.

As d increases so the windings of M^{u}_d and M^{s}_d become more pronounced. Figure 12*c* shows the situation for $d = 2.77$ and we shall devote the remainder of this section to that case, since it corresponds to a complex situation in which a strange attractor S_d apparently exists. Enlargements of portions of $M^{\mathrm{s}}_d \cup M^{\mathrm{u}}_d$ are also shown in figure 12*d*, the structure is shown schematically in figure 12*e* for clarity, and the behaviour of successive iterates of $P_d((x_0, y_0) = (0.0001, 0.0001))$ is shown in figure 13. After 10^6 iterates there is no convergence to a periodic orbit, but iterates rapidly approach M^{u}_d and it appears that M^{u}_d is closely related to (= identified with?) the expanding attractors $\mathscr{C}^{\pm}$ described above.

Finally one can view P_d as a 'horseshoe' map similar to those devised by Smale. In figure 14 we show a rectangle $R = \{x, y \mid |x| \leqslant 2, |y| \leqslant 0.4\}$ and its image $P^3_d(R)$ under three iterates of P. It is clear that P^3_d is identical to the map shown in figure 9*b*, apart from the reversal of orientation. P^3_d should thus share all the features of the horseshoe maps.

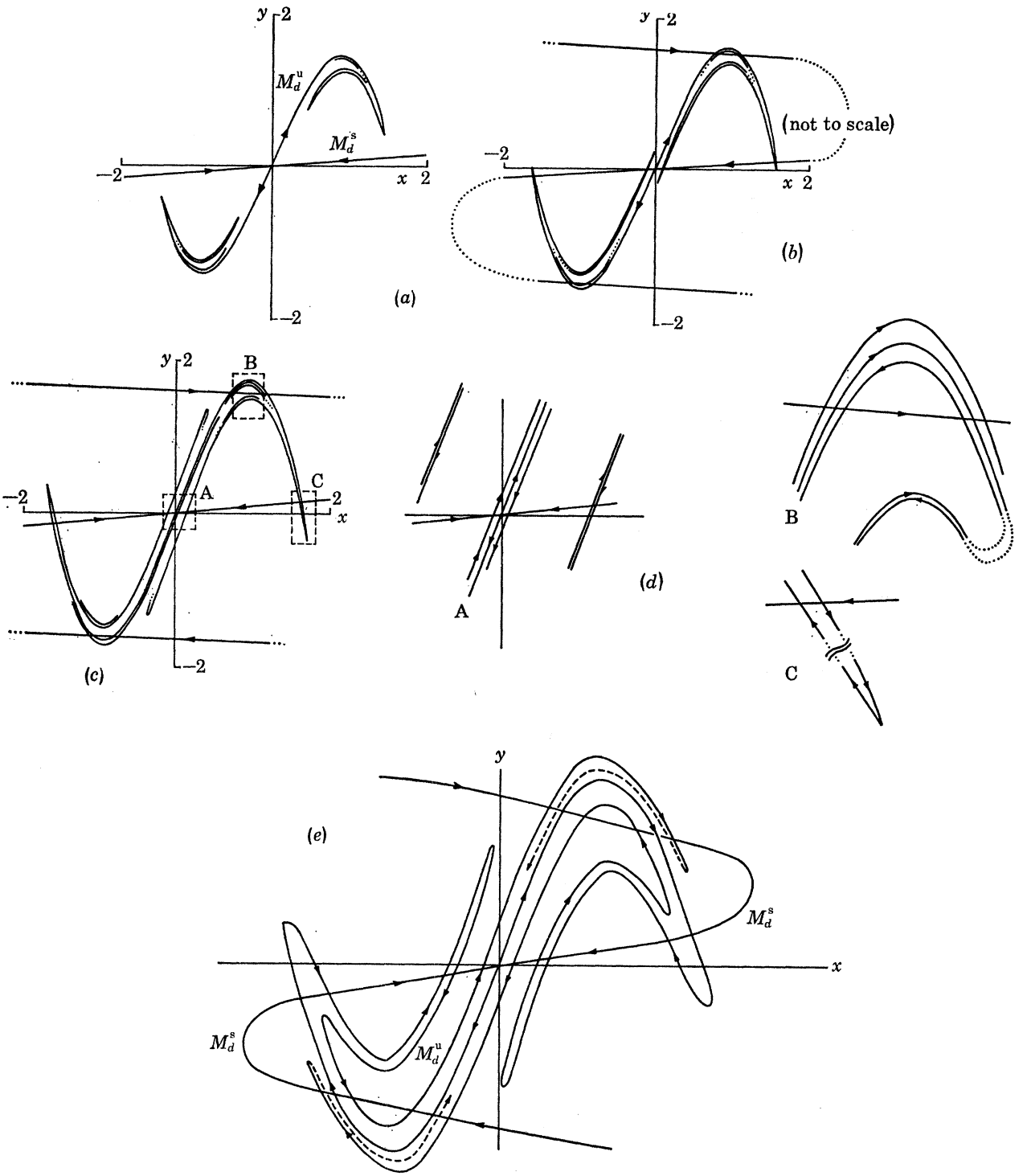

FIGURE 12. Portions of the stable and unstable manifolds M_d^u and M_d^s of (0, 0) for the map P_d; $b = 0.2$; (*a*) $d = 2.5$; (*b*) $d = 2.65$; (*c*) $d = 2.77$; (*d*) enlargements of regions A, B, C; (*e*) the structure of M_d^s and M_d^u for $d = 2.77$ (not to scale).

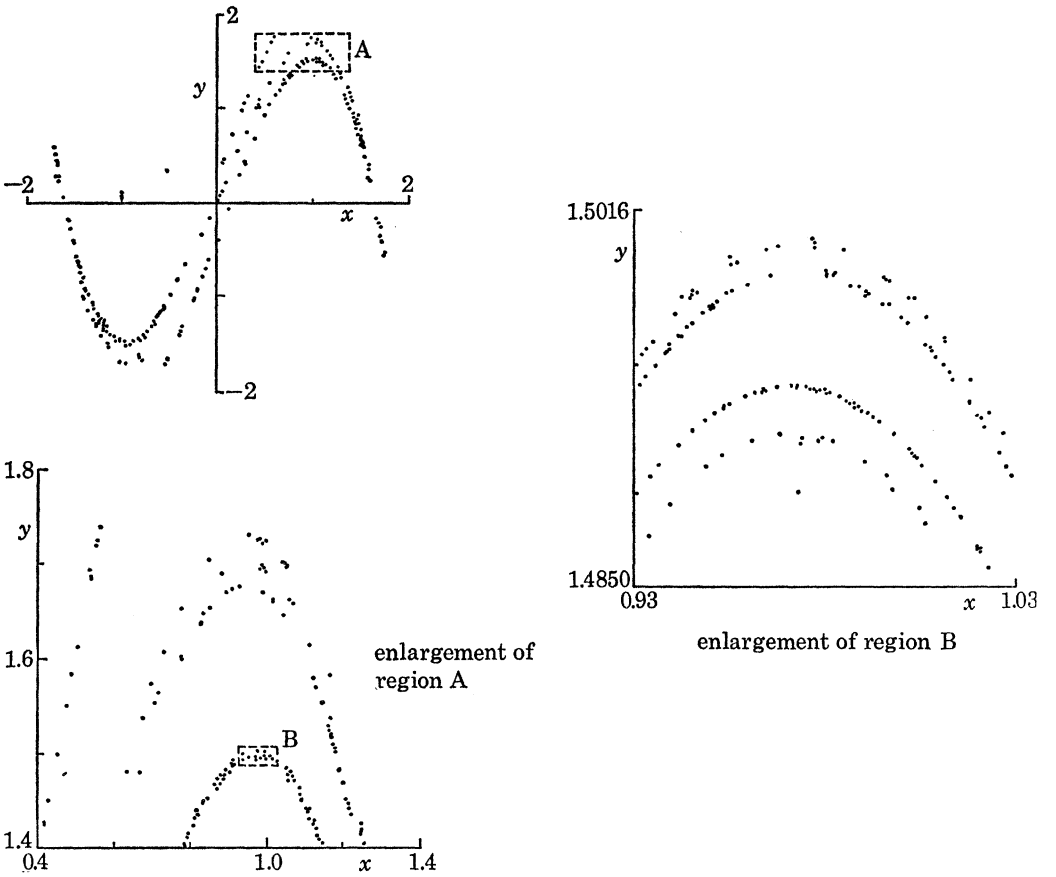

FIGURE 13. Successive iterates of P_d; $b = 0.2$, $d = 2.77$. Initial conditions $(x_0, y_0) = (0.0001, 0.0001)$.

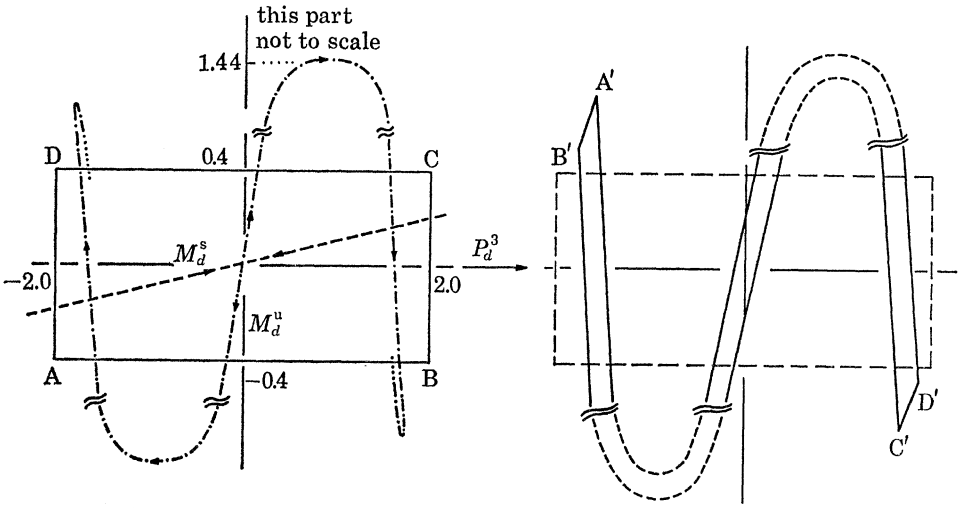

FIGURE 14. Global behaviour of P_d; $d = 2.77$.

5.3. *The structure of the attracting set S_d; $d = 2.77$*

In this section we collect all the relevant information on P_d derived so far and use it to obtain partial results and to make further conjectures on the structure of S_d.

For $d \lesssim 2.60$, P_d is relatively simple since there are no homoclinic points and almost all orbits converge to the fixed points or periodic orbits of period $2 (d \in (2.4, 2.58))$ or $4 (d > 2.58)$. For this situation we can represent the non-wandering set Ω of P_d as the union of a finite number of basic sets [3] $\Omega = \Omega_s \cup \Omega_1^+ \cup \Omega_1^- \cup \Omega_2^+ \cup \Omega_2^- \cup \ldots$ where Ω_s is the saddle point at $(0, 0)$, $\Omega_1^{\pm}$ are the (two) period 1 orbits (fixed points) at $(\pm (d-b-1)^{\frac{1}{2}}, \pm (d-b-1)^{\frac{1}{2}})$, $\Omega_2^{\pm}$ are the period two orbits etc. In fact here P_d satisfies Smale's Axiom A (Smale 1967; Chillingworth 1976), except at bifurcation values of d, since the non-wandering set Ω is hyperbolic and the periodic points are dense in Ω.

For $d \in (\approx 2.60, 2.70)$ we can make use of the same type of decomposition to obtain a non-wandering set $\Omega = \Omega_h \cup \Omega_1^+ \cup \Omega_1^- \cup \Omega_2^+ \cup \Omega_2^- \cup \ldots \cup \Omega_{2^n}^+ \cup \Omega_{2^n}^-$, for $n < \infty$. Here Ω_h represents the horseshoe of figures 9*b* and 14 arising as a result of the transversal homoclinic intersections of M_d^u and M_d^s.

Recall that Ω_h itself contains an infinite number of periodic points but that they are all of saddle type. Thus almost all orbits approach $\bigcup_{i=0}^{n} (\Omega_{2^i}^{\pm})$ or $\bigcup_{i=0}^{n} (\Omega_{2^i}^{-})$; moreover, recalling that $\Omega_{2^{n-1}}^{\pm}$ are all saddle type orbits, we can see that almost all orbits must approach the attracting orbits $\Omega_{2^n}^+$ or $\Omega_{2^n}^-$. The periodic points are still dense in Ω and, except at bifurcation values of d, they are hyperbolic. The complexity of the *transient* behaviour (cf. figures 11*d* and *e*) is due to the horseshoe Ω_h. The invariant set Ω_h is homeomorphic to the product of two Cantor sets $C \times C$ which is itself homeomorphic to C (cf. Chillingworth 1976, pp. 232–235). The outsets of Ω_h, which take the place of the unstable manifold M_d^u of Ω_s, also have a complicated structure which is locally homeomorphic to the product of a curve and a Cantor set. The distribution of the infinite number of periodic (saddle) points of Ω_h in the neighbourhood N of the original saddle $\Omega_s = (0, 0)$ is such that any two orbits with initial conditions arbitrarily close in N will eventually diverge. Thus the ultimate behaviour is particularly sensitive to initial conditions, although for $d \lesssim 2.70$ there are only two likely outcomes for any orbit: attraction to $\Omega_{2^n}^+$ or $\Omega_{2^n}^-$.

For $d \in (2.70, 2.75)$ the situation is only different in that the basic sets $\bigcup_{i=1}^{n} (\Omega_{2^i}^{\pm})$ develop attracting non-periodic orbits; in particular, they appear to contain orbits of arbitrarily high period $\{2^n l \mid n, l \to \infty, l \text{ odd}\}$ and ultimately orbits of periods $\ldots, 9, 7, 5, 3$ (see § 4.3). The behaviour associated with Ω_h remains distinct from the attracting motions. However, note that the attracting sets now appear to be one dimensional, since successive iterates of P_d move on the curves $\mathscr{C}^+$ and $\mathscr{C}^-$. Periodic points are presumably no longer dense and the system fails to be axiom A.

For $d \gtrsim 2.75$, and in particular for the case studied here of $d = 2.77$, the situation is critically different. We will try to reconstruct what happens. First denote the two branches of the global unstable manifold as M_d^{u+} and M_d^{u-}. For $d \lesssim 2.6$ M_d^{u+} runs from $(0, 0)$ to $\bigcup_{i=0}^{2} (\Omega_{2^i}^{+})$ and M_d^{u-} from $(0, 0)$ to $\bigcup_{i=0}^{n} (\Omega_{2^i}^{-})$. This presumably continues to hold for $d \in (2.6, 2.7)$, except that M_d^{u+} and M_d^{u-} now intersect M_d^s and the local structure of $M_d^{u+} \cup M_d^{u-}$, the outset of Ω_h, is

as described above. Thus, when the non-periodic motions in $\mathscr{C}^+$ and $\mathscr{C}^-$ replace the periodic attractors $\Omega^{\pm}_{2^m l}$ for $d \gtrsim 2.7$ we expect that M^{u+}_d runs from $(0, 0)$ to $\mathscr{C}^+$ and M^{u-}_d to $\mathscr{C}^-$. In fact $\mathscr{C}^+$ and $\mathscr{C}^-$ appear to be indistinguishable from the 'ends' of M^{u+}_d and M^{u-}_d away from $(0, 0)$. As d increases beyond 2.75, $\mathscr{C}^+$ and $\mathscr{C}^-$ are apparently 'drawn through' the stable manifold M^s_d in a manner such that orbits attracted to $\mathscr{C}^+$ (or $\mathscr{C}^-$) enter both the negative and positive half planes, as indicated in figure 13. Note that the iterates appear to lie on a set which locally has the structure of the product of a curve and a Cantor set, just as in the example discussed by Hénon (1976). Globally the set winds back and forth, approaching arbitrarily closely to the saddle at $(0, 0)$, and it is not clear whether it is a single curve (homeomorphic to $\mathbb{R}$) or whether two distinct curves $\mathscr{C}^+$ and $\mathscr{C}^-$ still exist.

The structure discussed above is, however, locally identical to that of the (generalized) unstable manifold of Ω_h, and it is possible that it is merely this that we observe, and orbits ultimately (after say 10^8 iterates!) converge upon periodic attractors. Moreover, Newhouse (1977) proves that if the stable and unstable manifolds of a hyperbolic basic set of a two dimensional diffeomorphism are tangent at some point, then there is a nearby open set of diffeomorphisms which possess *wild hyperbolic sets*. Wild hyperbolic sets are sets that contain infinitely many periodic sinks and in which persistent tangencies between stable and unstable manifolds occur. In the map P_d studied here the saddle point of period 1 at $(0, 0)$ is the basic set and since M^s_d and M^u_d are tangent for $d \approx 2.60$ we can conclude that wild hyperbolic sets exist for nearby values of d. In the computer studies we may therefore only be observing periodic motions of very long periods. In fact the C^0 density theorem (Smale 1971; Zeeman 1972) states that generically *under the C^0 topology* the only attractors likely to be found are fixed points and periodic orbits and thus that strange attractors and chaotic maps such as (4.8) are ruled out. Thus one might expect either (*a*) that P_d simply possesses periodic orbits of high period or (*b*) that if a nonperiodic attractor does exist, then an arbitrary small perturbation can destroy it and periodic orbits will appear in its place. However, the present results, those of Hénon (1976), and work on one dimensional maps such as (4.8 and 4.9) all strongly suggest that a non-periodic motion is present and that it cannot be removed by small perturbations. One is therefore led to question the use of the C^0 topology: intuitively it seems reasonable to demand that functions *and* (some of) their derivatives be close and not merely the functions themselves. Moreover, as Zeeman (1972) points out, the C^0 results do not extend easily to parameterised systems such as that considered here. In the C^1 topology strange attractors are encountered generically: for instance the Lorenz attractor is an example which has given rise to much work recently (Guckenheimer 1976, 1978; Rand 1978; Williams 1978).

In closing we note that even if almost all orbits of P_d (and of the o.d.e.) do ultimately approach stable periodic orbits, the periods appear to be so long that for all practical purposes they can be regarded as non-periodic motions.

5.4. *The implications for the o.d.e.*

We saw in § 2.3 how the Poincaré map $P: \mathbb{R}^2 \to \mathbb{R}^2$ captures and preserves the important features of the original o.d.e. or *flow* on $\mathbb{R}^2 \times S^1$: in particular periodic orbits of period n in the o.d.e. become periodic points or fixed points of P^n, the Poincaré map iterated n times. The non-periodic attractor S_d detected for P_d would thus correspond to a non-periodic orbit of the o.d.e., similar to the orbits observed in § 3. The similarity is even stronger: compare the qualitative structures of stable and unstable manifolds in figures 7*a–d* for the o.d.e. and figures

12*a–d* for P_d. The sequence of bifurcations occurring for P_d as d increases does not quite match that for the o.d.e. and global attraction is not preserved, but the general behaviour is very close. For an illustration of this, compare the time history $x(t)$ against t for the o.d.e. in figure 8*a* with the sequence of iterates x_i against i for the map P_d shown in figure 15*a*. In figure 15*b* we show the sequence for a lower value of d ($d = 2.71$) for which two distinct non-periodic attractors exist, as outlined in § 5.3 above: after about 40 iterates the orbit is captured by one of the attractors.

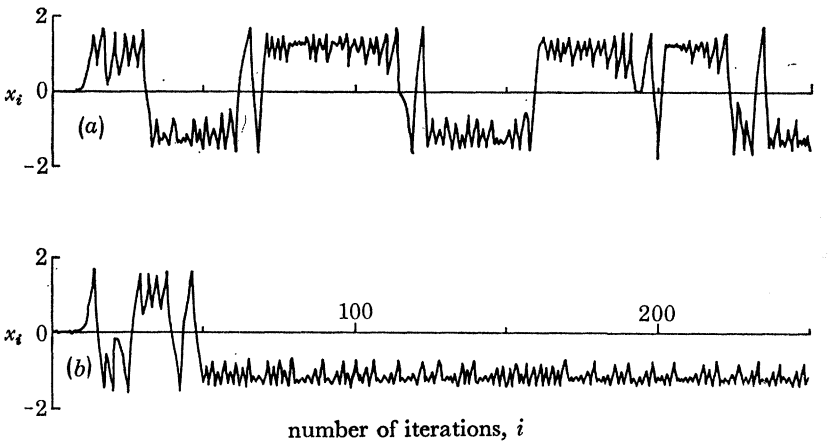

FIGURE 15. Time series of P_d; $b = 0.2$, initial conditions $(x_0, y_0) = (0.0001, 0.0001)$. Note non-periodic motions; (*a*) $d = 2.77$; (*b*) $d = 2.71$.

The *local* structure of the attracting set in the o.d.e. thus appears to be homeomorphic to the product of a two dimensional manifold and a Cantor set (the structure of P_d represents a local section transverse to the manifold). Thus its *local* structure is identical to that of the (geometric) Lorenz attractor (Guckenheimer 1976), while its *global* structure appears to be closely related to the winding of the stable and unstable manifolds M^s_d and M^u_d of the saddle point in the Poincaré map.

6. Conclusions and physical implications

In the paper we have analysed an apparently simple nonlinear oscillator which has relevance as a model for (small) lateral vibrations of certain buckled structures; in fact it applies to any situation in which the unforced system possesses two stable equilibria separated by a saddle point. We have studied the behaviour of such systems subjected to sinusoidal forced oscillations; the generalisation to arbitrary *periodic* forcing is natural and relatively straightforward cf. Morosov (1973, 1976). The simplicity of the o.d.e. is indeed only apparent; for certain parameter ranges we have shown that, while global stability is preserved in the sense that motions decay and all trajectories enter a closed region A in the state space, the structure of the invariant and attracting (sets) within A is extremely complex.

Making use of the work of Mel'nikov, we have proved that homoclinic motions occur within A if the external force amplitude f exceeds a critical level f_c, which we can compute approximately in specific cases. This implies that results obtained by conventional techniques such as the K–B averaging method are seriously in error qualitatively as well as quantitively. A number of other nonlinear oscillators are now known to possess homoclinic orbits, and it was

work on the van der Pol oscillator (Levinson 1949) which originally prompted Smale's construction of the horseshoe; cf. (Smale 1965). Holmes & Rand (1978) proved that the (autonomous averaged) 'variational' equation of the forced van der Pol oscillator possesses a homoclinic saddle connection. Since the actual system can be viewed as a periodic perturbation of the variational equation on $\mathbb{R}^2$, it would be natural to apply Mel'nikov's methods to study the creation of homoclinic orbits in the forced van der Pol system.

In the present case the homoclinic structure plays a critical part in the *attracting* motions appearing in A as f continues to increase. Our study of the nature of these is based upon analogue computer solutions of the o.d.e. and on analysis and digital computer studies of its Poincaré map P and an approximation, P_d, to P. While our conclusions on the structure of the attractors seem highly plausible, they cannot be regarded as proven.

For a range of values of d, P_d apparently possesses a strange attractor S_d which represents a cross section of the strange attractor S detected in analogue computer studies of the o.d.e. Locally S_d is homeomorphic to the product of a curve and a Cantor set, just as S is homeomorphic to the product of a two-manifold and a Cantor set. As $t \to +\infty$ all trajectories of the o.d.e. approach S, which is attracting and invariant under the flow of the o.d.e. (S contains all the periodic saddle type orbits created in successive bifurcations.) However, once on S the trajectories appear to move in the ergodic fashion dramatically illustrated in figures 8*a* and 15. Power spectra of such motions indicate a genuine persistence of non-periodic behaviour (figure 8*b*). The motions illustrated in figures 8*a* and 15*a* are particularly interesting, since here the systems oscillate irregularly between two states. There are two time scales apparent: relatively fast (almost periodic) oscillations close to the forcing frequency and slower, less regular, changes of state. The analysis above shows that the two are intimately connected. A number of physical problems exhibit differing time scales and two three dimensional systems have been proposed as models in this connection. The Rikitake dynamo (Cook & Roberts 1970) and related dynamos (Robbins 1977) have been suggested as models for reversals of the earth's magnetic field, and recent work on the p.d.e.s of magnetohydrodynamics suggests that such models may indeed be rigorously justifiable (Iooss & Lozi 1977). In studies o atmospheric turbulence (Bénard convection) Lorenz (1963) proposed a drastic truncation of the Overbeck–Boussinesq equations, which also possesses such chaotic dynamics. The Lorenz attractor has stimulated much of the mathematical work in the area. The present study suggests that similar phenomena may also arise in apparently simple mechanical systems undergoing forced oscillations.

We thus see that deterministic dynamical systems can give rise to motions which are essentially random. This has important implications in dynamical modelling exercises, as described previously (Holmes 1977*b*); in particular, qualitative information of the structure of attracting sets is essential if numerical simulations are to be attempted, since solutions with arbitrarily close initial conditions generally diverge after sufficient time and the behaviour superficially appears unstable. Perhaps more significantly, the generic existence of systems such as the present one suggests a new approach to a wide range of problems in which irregular oscillations are observed and in which they have traditionally been ascribed to the influence of stochastic forcing functions. If the ergodicity does arise as an intrinsic feature of the dynamics, then profound changes are necessary in concepts such as stability and repeatability.

Part of this work was done while the author held a research fellowship at the Institute of Sound and Vibration Research, Southampton University, U.K. He acknowledges financial assistance of the Science Research Council of the U.K. He would also like to thank Dr David Chillingworth, Dr David Rand and Professor Christopher Zeeman, F.R.S., for a number of stimulating and helpful discussions.

References

Arnold, V. I. 1964 *Soviet Math.* **5**, 584–585.
Baker, N. H., Moore, D. W. & Spiegel, E. A. 1971 *Q. Jl Mech. appl. Math.* **23**, 391–422.
Birkhoff, G. D. 1927 *Acta. Math., Soc.* 359–379.
Chillingworth, D. R. J. 1976 *Differential topology with a view to applications*. London: Pitman.
Cook, A. E. & Roberts, P. H. 1970 *Proc. Camb. phil. Soc.* **68**, 547–569.
Fiala, V. 1975 *Solution of nonlinear vibration systems by means of analogue computers*. Monographs and Memoranda of the National Research Institute for Machine Design, **19**, Behovice, Prague, Czechoslovakia.
Gavrilov, N. K. & Silnikov, L. P. 1972 *Math. USSR Sb.* **17** (4), 467–485.
Gavrilov, N. K. & Silnikov, L. P. 1973 *Math. USSR Sb.* **19** (1), 139–156.
Guckenheimer, J. 1976 *A strange, strange attractor*. §12 of Marsden & McCracken (1976).
Guckenheimer, J. 1978 *Proc. N.Y. Acad. Sci.* **316**, 78–85.
Hale, J. K. 1969 *Ordinary differential equations*. New York: John Wiley.
Hayashi, C., Ueda, Y. & Kawakami, H. 1969 *Int. Jl Nonlinear Mech.* **4**, 235–255.
Hayashi, C., Ueda, Y. & Akamatsu, N. & Itakura, H. 1970 *Electron. Commun. Jap.* **53** – A(3), 31–39.
Hayashi, C. & Ueda, Y. 1973 *Nonlinear Vib. Probl.* **14**, 341–351.
Hénon, M. 1976 *Commun. math. Phys.* **50**, 69–77.
Hirsch, M. W. & Smale, S. 1974 *Differential equations, dynamical systems and linear algebra*. London: Academic Press.
Hirsch, M. W., Pugh, C. C. & Shub, M. 1977 Invariant manifolds. *Springer Lect. Notes Math.* **583**. Berlin: Springer Verlag.
Holmes, P. J. 1976 *J. Sound Vib.* **49**, 607–611.
Holmes, P. J. 1977*a* *J. Sound Vib.* **53**, 471–503.
Holmes, P. J. 1977*b* *Appl. math. Model.* **1**, 362–366.
Holmes, P. J. 1979 *Proc. 17th I.E.E.E. Conf. on Decision and Control*, San Diego, CA, 10–12 January, 1979 paper WA 7, 181–185.
Holmes, P. J. & Marsden, J. E. 1978*a* *Automatica* **14**, 367–384.
Holmes, P. J. & Marsden, J. E. 1978*b* *Proc. N.Y. Acad. Sci.* **316**, 608-622.
Holmes, P. J. & Rand, D. A. 1976 *J. Sound Vib.* **44**, 237–253.
Holmes, P. J. & Rand, D. A. 1978 *Q. appl. Math.* **35**, 495–509.
Hsu, C. S. & Yee, H. C. 1975 *Trans. A.S.M.E. Jl appl. Mech.* **42**, 870–876.
Hsu, C. S., Yee, H. C. & Cheng, W. H. 1977*a* *Trans. A.S.M.E. Jl appl. Mech.* **44**, 147–155.
Hsu, C. S., Yee, H. C. & Cheng, W. H. 1977*b* *J. Sound Vib.* **50**, 95–116.
Huang, N. C. & Nachbar, W. 1968 *Trans. A.S.M.E. Jl appl. Mech.* **35**, 289–297.
Iooss, G. & Lozi, R. 1977 *J. Méc.* **16**, 675–703.
Levinson, N. 1949 *Ann. math.* **50**, 127–153.
Li, T. Y. & Yorke, J. A. 1975 *Am. math. Mon.* **82** (10), 985–992.
Lorenz, E. N. 1963 *J. atmos. Sci.* **20**, 130–141.
Lorenz, E. N. 1964 *Tellus* **16**, 1–11.
Markus, L. 1971 *Lectures in differentiable dynamics*. Amer. Math. Soc. Regional Conference Series no. 3, Providence, R.I.
Marsden, J. E. & McCracken, M. 1976 *The Hopf Bifurcation and its Applications*. Springer Applied Math. Series, no. 19. Berlin: Springer-Verlag.
May, R. M. 1974 *Science, N.Y.* **186**, 645–647.
McGehee, R. & Meyer, K. 1974 *Am. J. Math.* **96**, 409–421.
Mel'nikov, V. K. 1963 *Trans. Moscow math. Soc.* **12** (1), 1–57.
Morosov, A. D. 1973 *USSR comput. Math. math. Phys.* **13** (5), 45–66.
Morosov, A. D. 1976 *Diffl. Eqns.* **12**, 164–174.
Newhouse, S. 1977 *The abundance of wild hyberbolic sets and nonsmooth stable sets for diffeomorphisms*. Bures-sur-Yvette, Paris: Institute des Hautes Etudes Scientifiques.
Nitecki, Z. 1971 *Differentiable dynamics*. Cambridge, Mass.: M.I.T. Press.
Poincaré, H. 1899 *Les Methodes Nouvelles de la Mechanique Celeste*, vol. III. Paris. (Reprinted by Dover, 1957).
Rand, D. A. 1978 *Math. Proc. Camb. Phil. Soc.* **83**, 451–460.
Robbins, K. A. 1977 *Proc. natn. Acad. Sci. U.S.A.* **73**, 4297–4301.

PHILOSOPHICAL TRANSACTIONS OF THE ROYAL SOCIETY A MATHEMATICAL, PHYSICAL & ENGINEERING SCIENCES

Ruelle, D. 1978 *Proc. N.Y. Acad. Sci.* **316**, 408–416.
Ruelle, D. & Takens, F. 1971 *Communs math. Phys.* **20**, 167–192; **23**, 343–344.
Šarkovskii, A. N. 1964 *Ukr. mat. Zh.* **16**, 61–74 (in Russian).
Smale, S. 1963 *Proc. Int. Symp. Nonlinear Vibrs* II, 1961, *Izdat. Akad. Nauk., Ukraine SSR*, Kiev.
Smale, S. 1965 In *Differential and combinational topology* (ed. S. S. Cairns), pp. 63–80. Princeton University Press.
Smale, S. 1967 *Bull. Am. math. Soc.* **73**, 747–817.
Smale, S. 1973 In *Proc. Int. Symp. Dynamical Systems*, Salvador, Brazil (ed. M. M. Peixoto), pp. 527–530.
Stefan, P. 1977 *Communs math. Phys.* **54**, 237–248.
Tondl, A. 1976 *On the interaction between self-excited and forced vibrations*. Monographs and Memoranda of the National Research Institute for Machine Design **20**, Bechovice, Prague, Czechoslovakia.
Ueda, Y., Hayashi, C. & Akamatsu, N. 1973 *Electron. Communs. Jap.* **50** – A (4), 27–34.
Williams, R. 1978 *Proc. N.Y. Acad. Sci.* **316**, 393–399.
Zeeman, E. C. 1972 *Proc. Colloq. on Smooth Dynamical Systems*, Southampton, September 1972, pp. 18–20.

PHILOSOPHICAL TRANSACTIONS OF THE ROYAL SOCIETY A MATHEMATICAL, PHYSICAL & ENGINEERING SCIENCES